

SCUOLA DI SCIENZE

Dipartimento di Chimica Industriale "Toso Montanari"

Corso di Laurea Magistrale in

**Chimica Industriale**

Classe LM-71 - Scienze e Tecnologie della Chimica Industriale

**Chemical composition modification of casting  
aluminium alloys for engine applications**

Tesi di laurea sperimentale

**CANDIDATO**

Alessandro Graziani

**RELATORE**

Chiar.mo Prof. Alessandro Morri

**CORRELATORI**

Stefania Toschi

Lorella Ceschini

Andrea Morri

**III Sessione**

---

**Anno Accademico 2014-2015**

---

# Contents

## Abstract

<b>Chapter 1 – Introduction</b>	1
<b>1.1 An introduction on aluminium</b>	1
<b>1.2 Aluminium alloys</b>	2
<b>1.2.1 Casting alloys</b>	2
<b>1.2.2 Aluminium-silicon alloys</b>	4
<b>1.2.3 State of the art on alloying elements of Al-Si alloys</b>	7
<b>1.3 Heat treatments</b>	11
<b>1.3.1 Heat treatments of Al-Si-Cu-Mg and Al-Si-Mg alloys</b>	14
<b>1.4 Thermal stability of precipitates</b>	18
<b>1.4.1 Change of composition for high temperature applications</b>	19
<b>1.5 Aim of the research</b>	25
<b>Chapter 2 – Material and method</b>	26
<b>2.1 Material</b>	26
<b>2.2 Mould preparation</b>	26
<b>2.3 Casting</b>	27
<b>2.4 Chemical analysis</b>	29
<b>2.5 Heat treatment</b>	30
<b>2.6 High temperature exposure</b>	32
<b>2.7 Hardness measurement</b>	32
<b>2.8 Metallographic analysis</b>	33
<b>2.9 Secondary Dendrite Arm Spacing (SDAS) measurement</b>	34
<b>2.10 Thermal analysis</b>	35
<b>2.11 Tension tests</b>	35
<b>2.12 Fractography</b>	37
<b>Chapter 3 – Results</b>	38

<b>3.1 Thermal analysis</b>	38
<b>3.2 Heat treatment</b>	38
<b>3.3 Metallographic analysis</b>	39
<b>3.3.1 Optical microscopy</b>	39
<b>3.3.1.1 A354 alloy</b>	39
<b>3.3.1.2 A354 + 0.1%Mo (casting sequence A)</b>	40
<b>3.3.1.3 A354 + 0.3%Mo (casting sequence A)</b>	41
<b>3.3.1.4 A354 + 0.3%Mo (casting sequence B)</b>	42
<b>3.3.1.5 A354 + 0.5%Mo (casting sequence A)</b>	43
<b>3.3.1.6 A354 + 0.8%Mo (casting sequence A)</b>	44
<b>3.3.2 Scanning electron microscopy</b>	45
<b>3.3.2.1 Aluminium-molybdenum master alloy</b>	45
<b>3.3.2.2 A354 + 0.1%Mo (casting sequence A)</b>	45
<b>3.3.2.3 A354 + 0.3%Mo (casting sequence A)</b>	48
<b>3.3.2.4 A354 + 0.3%Mo (casting sequence B)</b>	50
<b>3.4 Secondary Dendrite Arm Spacing (SDAS) measurement</b>	52
<b>3.5 Hardness measurements</b>	52
<b>3.5.1 Macrohardness measurements</b>	52
<b>3.5.2 Microhardness measurements</b>	54
<b>3.6 Ageing curves</b>	55
<b>3.7 High temperature exposure</b>	56
<b>3.7.1 Solution treatment 495°C for 6h + 540°C for 1h + soaking 245°C for 301h</b>	56
<b>3.7.2 Solution treatment 495°C for 6h + 540°C for 1h + soaking 245°C for 120h + 300°C for 42h</b>	58
<b>3.7.3 Solution treatment 495°C for 6h + 540°C for 1h + soaking 245°C for 301h</b>	60
<b>3.8 Tension tests</b>	61
<b>3.9 Fractography</b>	62
<b>Chapter 4 - Conclusions</b>	65
<b>Appendix</b>	66
<b>References</b>	75
<b>Acknowledgments</b>	77

## Abstract

The research activities were focused on evaluating the effect of Mo addition to mechanical properties and microstructure of A354 aluminium casting alloy.

Samples, with increasing amount of Mo, were produced and heat treated.

After heat treatment and exposition to high temperatures samples underwent microstructural and chemical analyses, hardness and tensile tests.

The collected data led to the optimization of both casting parameters, for obtaining a homogeneous Mo distribution in the alloy, and heat treatment parameters, allowing the formation of Mo based strengthening precipitates stable at high temperature.

Microstructural and chemical analyses highlighted how Mo addition in percentage superior to 0.1% wt. can modify the silicon eutectic morphology and hinder the formation of iron based  $\beta$  intermetallics.

High temperature exposure curves, instead, showed that after long exposition hardness is slightly influenced by heat treatment while the effect of Mo addition superior to 0,3% is negligible.

Tensile tests confirmed that the addition of 0.3%wt Mo induces an increase of about 10% of ultimate tensile strength after high temperature exposition (250°C for 100h) while heat treatments have slight influence on mechanical behaviour.

These results could be exploited for developing innovative heat treatment sequence able to reduce residual stresses in castings produced with A354 modified with Mo.

## Riassunto

L'attività di tesi è stata incentrata sullo studio dell'effetto della presenza di Mo sulle prestazioni meccaniche e sulla microstruttura della lega di alluminio da fonderia A354.

Per tale ragione sono stati prodotti getti in lega A354 contenenti livelli crescenti di Mo, che dopo aver subito diversi trattamenti termici sono stati prima esposti ad alte temperatura e quindi sottoposti ad analisi microstrutturali, chimiche, a prove di durezza e trazione.

Lo studio ha permesso di definire sia i parametri del processo di colata per ottenere un' omogenea distribuzione del Mo nella lega solidificata, sia quelli del trattamento termico al fine di potere ottenere un rinforzo per precipitazione dovuto alla formazione di dispersoidi a base Mo stabili alle alte temperature.

Le analisi microstrutturali e chimiche hanno inoltre evidenziato come l'aggiunta di Mo in percentuali superiori allo 0.1% induca sia un effetto positivo dovuto al mancato sviluppo di precipitati  $\beta$  a base Fe sia un effetto negativo legato alla mancata sferoidizzazione del Si eutettico.

Le curve di degrado hanno invece evidenziato come dopo lunghi periodi di esposizione in temperatura le durezze del materiale non sia influenzata dalla percentuale di Mo aggiunta alla lega quando supera lo 0.3% e solo leggermente dal trattamento termico.

Le prove di trazione hanno confermato che l'aggiunta di Mo (pari a 0.3%) determina un incremento della resistenza della lega dopo esposizione prolungata a 250°C per 100h di circa il 10%. Come per le durezze anche la resistenza a trazione, dopo esposizione in temperatura, appare poco influenzata da modifiche dei parametri di trattamento termico. Questo permetterebbe di valutare la possibilità di utilizzare sequenze di trattamento termico della lega con Mo in grado di ridurre le tensioni residue nei getti senza penalizzarne la resistenza.

# Chapter 1 - Introduction

## 1.1 An introduction on aluminium

Aluminium is the third most abundant element on Earth's crust after oxygen and silicon, but nevertheless its manufacture and use were limited up to XIX century.

In fact only in 1807 its existence was postulated by the English chemist Davy, while it was produced (even if in small quantities) for the first time by the Danish Oersted in 1825.

But the interest for this metal aroused only after 1845, the year in which the German Wohler proved some properties of the new material including lightness.

Subsequently more and more efficient production processes were developed, starting from the thermo-chemical one by Sainte-Claire Deville (which was so costly that aluminium was even more expensive than gold) to the electrolytic by Hall and Heroult (1886), then improved and patented by the Bayer in 1888 [1].

The main properties of aluminium are [1]:

- Low density ( $2.7 \text{ g/cm}^3$ )
- High intrinsic resistance and Young's modulus (that is related with material density)
- Ductile behaviour even at low temperature
- Elevated corrosion resistance (thanks to the formation of a thin layer of protective oxide on its surface)
- Good deformability and machinability
- High malleability
- Elevated electrical conductivity (if related with metal density is even bigger than that of copper)
- Good thermal conductivity
- High riciclability

Thanks to these properties today aluminium alloys are more and more employed in many areas, particularly that of transports.

One of the most important sector is that of automotive, in which these materials have been finding many applications during the years (for example chassis, motor elements and wheel rims manufacture), allowing to substitute materials like steel and cast iron, contributing to reduce vehicles weight greatly and then also fuel consumptions and emissions [2].

## **1.2 Aluminium alloys**

Primarily aluminium alloys can be distinguished in two categories: wrought and cast alloys.

The first ones are casted as ingot or billet and then mechanically worked by processes such as rolling or extrusion to final form.

Cast alloys instead are manufactured directly to final or near final form without any mechanical working.

The wrought and casting alloys, their properties, nomenclature and applications are definitely different [1].

Inside every category it's possible to further distinguish every alloy series on the basis of the capability of undergoing a heat treatment, which guarantees an improvement of mechanical properties by precipitation of secondary phases.

Relatively to non-heat treatable alloys their performances can be enhanced by adding the aluminum with other alloying elements (both for wrought and casting alloys) or through various degrees of cold working or strain hardening (just for wrought ones) [1].

### **1.2.1 Casting alloys**

Aluminium is widely employed in foundry as a consequence of [1]:

- Low melting point
- High molten metal fluidity
- Good superficial finish
- Low gas solubility (except hydrogen)

At the same time foundry alloys show a series of problems, which reduce their properties.

The most important ones are high solidification shrinkage and thermal expansion coefficient, as well as hydrogen absorption, which cause the development of stress, voids and cracks (for example “hot tears”) [1].

Pure aluminium is not usually used for structural applications because of its low hardness, Young’s modulus and wear resistance, as well as absence of fatigue limit.

So, in order to produce a material of adequate strength for manufacturing structural components, it is necessary to add other elements to it, which allow producing a selection of different alloys, that can be used in a wide assortment of structural applications [3].

Casting alloys could be distinguished according to their composition in different series by using IADS (International Alloy Designation System) nomenclature [1]:

- 1xx.x - Pure aluminium – It shows elevated corrosion resistance and machinability, but it’s characterised by very low mechanical properties and can’t undergo heat treatments.

Applications: Food and chemical industries, electrical cable

- 2xx.x - Al-Cu – The addition of copper increases mechanical properties (especially after heat treatment) and makes heat treatable the alloy.

Otherwise this series is affected by low fluidity and ductility as well as corrosion resistance (in fact it’s susceptible to stress-corrosion cracking).

Applications: cylinder heads for automotive and aircraft engines, pistons for diesel engines, exhausting system parts.

- 3xx.x - Al-Si-Cu/Al-Si-Mg – This series is heat treatable and shows high mechanical performances and good fluidity and wear resistance.

At the same time copper-containing alloys show good machinability but also decreased corrosion resistance.

Applications: automotive cylinder blocks and head, car wheels, aircraft fittings, casings and other parts of compressors and pumps.

- 4xx.x - Al-Si – The presence of silicon induces high fluidity, moderate strength and ductility, good wear and corrosion resistance.

Otherwise these alloys can’t undergo heat treatment.

Applications: pump casings, thin wall castings, cookware.

- 5xx.x - Al-Mg – By adding magnesium to pure aluminium, it's possible to reach the optimal compromise between mechanical and corrosion resistance. It's characterised by moderate cast properties and good machinability and shows good appearance when anodized.

Applications: car wheels, pressure vessels, chemical plants

- 7xx.x - Al-Zn – The presence of zinc generates good dimensional stability and corrosion resistance and makes the heat treatment possible.

Otherwise this series shows low fluidity and cast properties.

Applications: aircraft parts

- 8xx.x - Al-Sn – This non heat treatable series demonstrates high wear resistance and good machinability, but very low mechanical properties.

Applications: anti-friction components

- 9xx.x – Other compositions

(The last “x” after the point shows if the material is used for castings if x=0 or for ingots if x=1)

### **1.2.2 Aluminium-silicon alloys**

One of the most commonly used alloying elements in casting alloys, thanks to the properties induced to aluminium and the capability of counterbalancing the detrimental effects of cast alloys is silicon.

Al-Si alloys are employed in many different foundry processes such as the sand, die and investment casting [1].

In fact this element guarantees [1]:

- High castability
- Low thermal expansion coefficient
- High thermal and electric conductivity

- Good mechanical properties and hardness
- High corrosion and wear resistance
- Possibility of being heat treated (in combination with adequate alligants)

These features allow the wide use of Al-Si alloys in many sectors such as automotive and aeronautic ones.

As it was said before one of the greatest problems for cast alloys is the presence of defects (resulting both from solidification and casting itself).

Therefore the use of silicon is significant since it increases the molten metal fluidity, which results in a better mold filling and in a consequent reduction of internal casting defects, while reduces the thermal expansion coefficient (which induces stresses and cracks) and enhances corrosion resistance [1].

According to silicon content inside the matrix it's possible to distinguish hypoeutectic (5-10 % Si), eutectic (11-13%) and hypereutectic (14-20%).

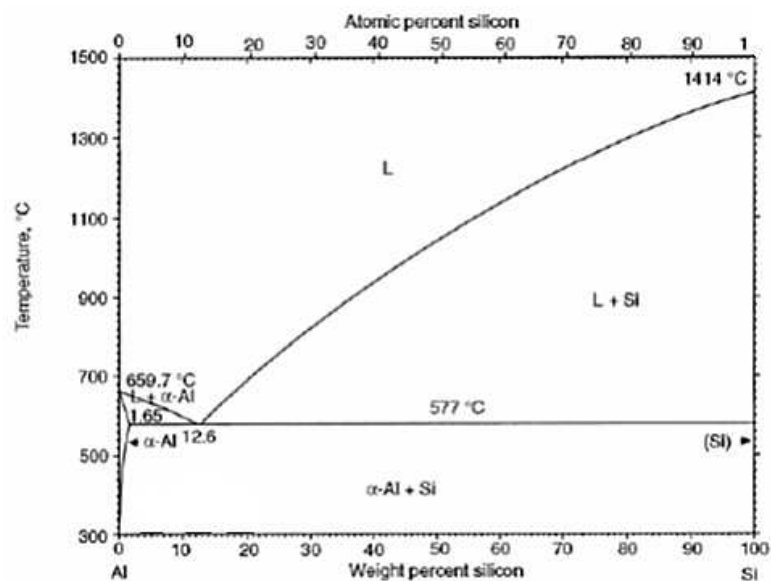


Figure 1 – Aluminum-silicon phase diagram [4]

As it could be observed in Al-Si phase diagram reported in fig. 1 pure aluminium melts at 660°C and silicon at 1414°C, while at 577°C and for a content of the latter equal to 12.6% wt. eutectic point is recorded.

About solubilities it could be stated that the silicon's one in aluminium is really low due to the limited extension of the area corresponding to  $\alpha$ -phase (that is pure aluminium),

while that of the second element in the first one is fairly nil and this causes primary silicon formation already for low weight percentages of the latter.

Hypoeutectic alloys are employed due to their good castability and corrosion resistance and are characterised by a microstructure made up of  $\alpha$ -Al dendrites (corresponding to the white regions of the photograph on the left in fig. 2) and eutectic Al-Si (identified by darker areas).

The hypereutectic alloys instead show a better fluidity, an excellent corrosion resistance and a fairly good thermal conductivity.

Their microstructure is mainly composed by particles of primary silicon (identified by big and dark areas in the photograph on the right in fig. 2) enclosed by a matrix formed by eutectic Al-Si.

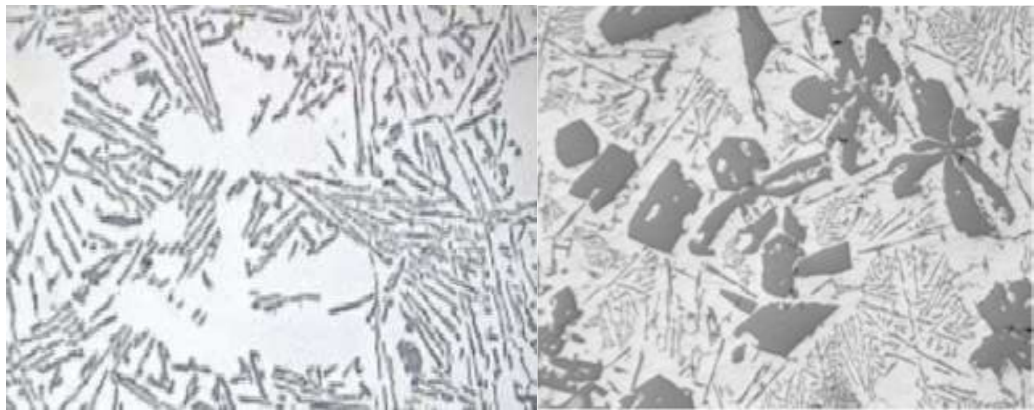


**Figure 2 – Images by optical microscope of the microstructures of a hypoeutectic (on the left) and hypereutectic (on the right) Al-Si alloy at 100x magnification [3]**

Anyway the properties of Al-Si alloys depend closely on dimension, morphology and distribution of silicon rather than only on his content.

As seen before the morphology of the eutectic silicon particles is generally needle or plate-like and the primary silicon particles are large and faceted, producing stress concentrations that degrade the mechanical properties of the material. Therefore, it's usually applied a chemical modification to refine the size of these particles and to change their morphologies, enhancing consequently alloy ductility [1].

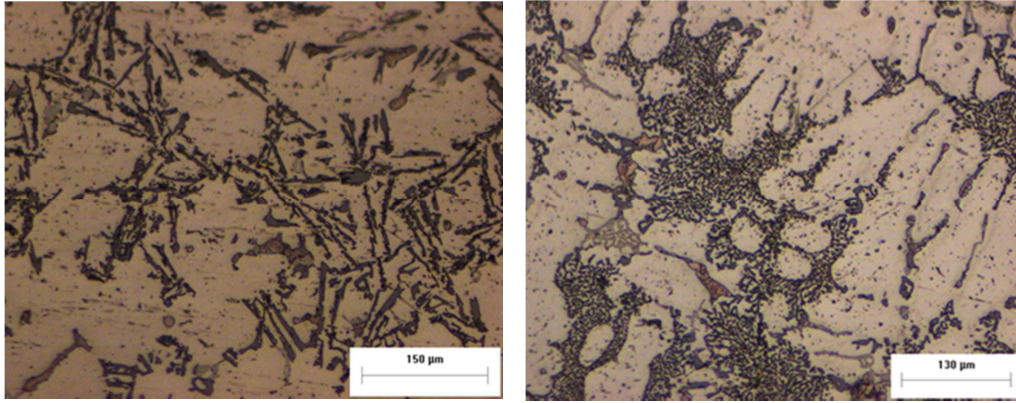


**Figure 3 – Images by optical microscope of the microstructures of hypoeutectic Al-Si unmodified (on the left) at 50x magnification and modified with strontium (on the right) at 20x magnification**

Nevertheless the use of strontium is preferred to that of sodium, because the latter is more reactive and less stable at high temperature present inside molten metal than the former, so it's not possible to define exactly its content inside the alloy and the effects of sodium fade relatively rapidly (overall when the molten metal is held at temperature for a prolonged period before solidification).

### **1.2.3 State of the art on alloying elements of Al-Si alloys**

To increase the performance (particularly at high temperature), the addition of further alligants able to create a series of intermetallics (during solidification phase or due to precipitation as a consequence of heat treatment) is necessary [1].

The criteria by which choose the alloying elements for Al-Si alloys are [4]:

- Development of a reinforce phase
- Low solubility in solid phase
- Low diffusivity in matrix
- Low influence on alloy castability

Nowadays the most commonly used alloying elements are as follows:

- **Copper** – It provides substantial increases in mechanical and fatigue resistance and hardness and facilitates precipitation hardening.

The introduction of copper to aluminium can also reduce ductility and corrosion resistance, while the susceptibility to solidification cracking (the so-called “hot tears”) is increased.

It’s usually present at percentages between 0.5 and 5.5% wt. [1].

- **Magnesium** - The addition of magnesium (0.6-1.3% wt.) to aluminium enhances corrosion resistance and hinders hydrogen absorption (especially after heat treatment), but on the other hand it increases thermal expansion and reduces ductility [1].

Silicon alone in aluminium produces a non-heat-treatable alloy. However in combination with magnesium and copper it generates a precipitation hardening heat-treatable alloy and so it’s possible to increase the properties of the base alloy, but at the same time this reduces ductility, corrosion resistance and molten metal fluidity.

- **Tin** – Tin is mainly employed because of its capability of improving tribological behaviour, by reducing friction, but also thanks to the higher machinability it gives to alloys [1].
- **Iron** – Iron is always available in alloys even if it’s usually considered an impurity, so in most alloys efforts are made to keep it as low as economically possible. In fact it causes alloy embrittlement, porosity increase and reduces castability, corrosion resistance, ductility and toughness.



Figure 4 – Microstructure of an as-cast hypoeutectic alloy containing  $\beta$ -Al<sub>5</sub>FeSi phase

Nevertheless it's added to particular alloys (may be added deliberately up to 3% Fe), which need hardness and high temperature resistance increases and the disadvantages of iron are not important or are counterbalanced by other elements (for example manganese and chromium) [1].

- **Manganese** – It's usually considered an impurity and so is maintained at low percentages in high quality components.

However it can be used as a modifier of needle-like iron intermetallics, in fact these change their morphology from  $\beta$  to  $\alpha$ -phases, increasing alloy ductility and reducing casting defects.

A high volume fraction of  $MnAl_6$  in alloys containing more than 0.5% in manganese can improve mechanical resistance.

Finally it can be employed to improve anodizing finish [1].

- **Zinc** – In combination with copper and/or magnesium allows the enhancement of mechanical properties by precipitation hardening after heat treatment [1].

- **Titanium** – Titanium is added at percentages of about 0.1-0.2% to aluminium primarily as a grain refiner. This effect is enhanced if boron is present in the melt or if it is added as a master alloy containing it.

In fact fine  $TiAl_3$  nuclei can be covered by compounds such as  $TiB_2$  and  $(Ti, Al)B_2$ , which promotes the deposition of aluminum on nuclei themselves, generating fine grains [1].

- **Lithium** - The addition of lithium to aluminium can substantially increase strength and Young's modulus, provide precipitation hardening and decreases density.

In fact every 1% by weight of lithium added to aluminum reduces the density of the resulting alloy by 3% and increases the stiffness by 5%. This effect works up to the solubility limit of lithium in aluminum, which is 4.2%.

Nevertheless the addition of lithium causes the reduction of ductility and fracture toughness[1].

- **Chromium** – It increases the corrosion resistance and modifies the morphology of iron intermetallics, increasing the ductility of the alloy, as well as allows grain refinement.  
Otherwise its addition strongly reduces molten metal fluidity, causing subsequently internal casting defects [5].
- **Cobalt** – Cobalt is mainly utilised for his beneficial effect on iron intermetallics. In fact it modifies their morphology from  $\beta$  to refined and distributed  $\alpha$ -phases, increasing ductility and mechanical resistance of the alloys [6].

In Al-Si-Cu-Mg series the most commonly used hypoeutectic alloys are A319, A356 and A354 (the last of which was the focus of the study).

The considered alloys are characterised by different compositions, which are described in the table below:

	%Si	%Cu	%Mg	%Fe	%Mn	%Ti	%Ni	%Zn
<b>A319</b>	5.5 – 6.5	3 - 4	≤ 0.1	≤ 1.0	≤ 0.5	≤ 0.25	≤ 0.35	-
<b>A354</b>	8.6 – 9.5	1.6 - 2	0.4 – 0.6	≤ 0.2	≤ 0.1	≤ 0.2	-	≤ 0.1
<b>A356</b>	6.5 – 7.5	≤ 0.2	0.2 – 0.4	≤ 0.2	≤ 0.1	≤ 0.2	-	≤ 0.1

**Table 1 – Compositions of A319, A354 and A356 alloys with percentages of alloying elements [7, 8]**

The different compositions obviously affect the alloys features.

In fact compared to A319 alloy A354 and A356 ones exhibit higher molten metal fluidity, shrinkage and hot cracking resistance (anyway all the alloys demonstrate high values for these parameters), while corrosion resistance is elevated in A356 alloy and moderate in the other ones.

Also mechanical properties show substantial differences.

In the table below some data are reported to illustrate how alloys composition influences their behaviour:

	Young's modulus (Gpa)	Yield strength (MPa)	Ultimate tensile strength (Mpa)	Elongation (%)
A319	74	90 - 95	155 - 195	2 - 3
A354	73	250 - 310	320 - 380	2 - 5
A356	73	190 - 250	260 - 275	3 - 10

**Table 2 – Mechanical characterisation of A319, A354 and A356 alloys [7, 8]**

Observing the table, it's possible to see that Young's modulus values are fairly identical, while the other parameters show substantially different ones.

In fact A319 alloy is characterised by the lowest values in resistance, but at the same time undergoes the lowest deformation. Conversely among these alloys A354 one exhibits the highest mechanical resistance, whilst A356 one the biggest deformation [7, 8].

Finally, as each considered alloy is heat-treatable, it should be remembered that the values reported above can be further modified and increased by specific treatment.

Anyway as a consequence of their features these alloys apply to different fields.

A319 alloy is employed in engine parts (for example cylinder heads), gasoline and oil tanks.

On the contrary some A356 typical applications are cylinder heads, wheels, engine support pylon, truck chassis parts, aircraft (for example wing flaps) and missile components.

Finally research on A354 alloy has been begun during last years and has been focused on its employment in engine parts [7,8].

### **1.3 Heat treatments**

Heat treatment is a process conducted to develop desirable mechanical properties required for service performance.

According to their composition alloys could be heat-treated or not.

For example, considering cast alloys, 2xx, 3xx, 7xx and 8xx alloys are heat-treatable, while 1xx, 4xx, 5xx and 9xx not.

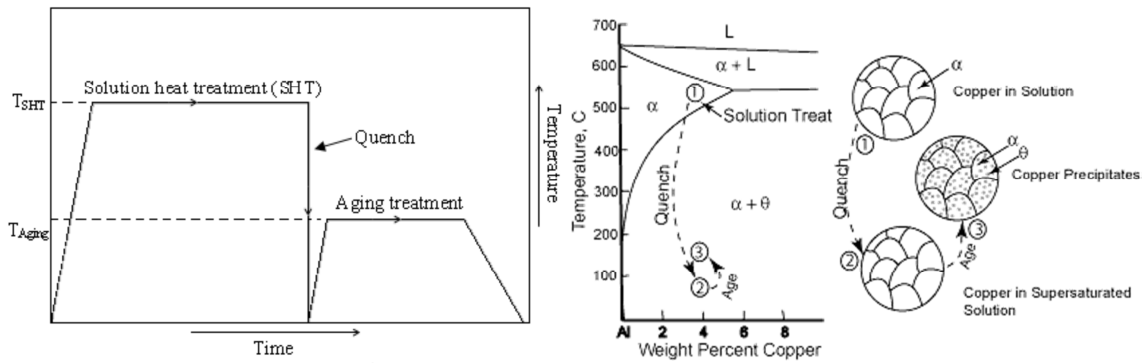


**Figure 5 – General schemes of heat treatment of aluminum alloys. In particular the image on the right shows the effects of the process on the microstructure of copper-containing alloys [10]**

Aluminium heat treatments are usually divided in 3 stages: solution, quenching and ageing.

The most commonly used heat-treatment for aluminum alloys is T6, which induces the highest hardness, wear resistance, mechanical properties and consists of a primary solution phase, followed by rapid cooling and artificial ageing [9,10].

- Solution treatment

Solution treatment involves heating the alloy to a temperature just below the lowest melting point of the alloy system (usually between 500 and 550°C), holding at this temperature until the base metal dissolves a significant amount of the alloying elements and becomes homogeneous.

The control of temperature and time is fundamental, because, if duration is too short not all alloying elements added will be dissolved and made available for precipitation hardening, while if too long more energy than necessary will be used and grain growth and overheating will develop [9,10].

- Quench

After that the alloy is rapidly cooled to retain as much of the alloying elements in solution as possible and so produces a supersaturated solid solution, that is an unstable condition in which the alligants exceed the solid solubility limit at room temperature.

The objectives of quench are to retain the maximum amount of the precipitation hardening elements in solution to form a supersaturated solid solution at low

temperatures and to suppress precipitation during rapid cooling of the casting from the high solution treatment temperature.

Cooling rates should be selected to retain as much solute as possible in solid solution, minimize component distortion and reduce the duration time over certain critical temperature ranges, avoiding diffusion of smaller atoms, which can lead to the precipitation.

In fact a slow rate of cooling would reduce residual stresses and distortion in the components, however it causes detrimental effects such as: precipitation during quench, localized over-ageing, increase tendencies for corrosion and result in a reduced response to ageing treatment due to the reduction in supersaturation of solute [9,10].

- Ageing

Then the last phase is characterised by the precipitation of intermetallics, which exploits the previous supersaturation and could be developed “naturally” at room temperature or promoted artificially by heating the alloy at a range temperature between 120-200°C.

The precipitation stage can be divided in: supersaturated solid solution → formation of GP zones → coherent precipitates → semi-coherent precipitates → incoherent precipitates

(the length of each step in the sequence depends on the thermal history, the alloy composition and the aging temperature) [9]

After solution treatment and quenching the matrix has a high super-saturation of solute atoms.

Clusters of atoms form rapidly from the supersaturated matrix and evolve into GP zones. From GP zones metastable coherent precipitates form (indicated by “ after the letter identifying the phase), which thanks to the high degree of coherency with matrix give great strengthening to the material.

As ageing proceeds, the coherent precipitates start to dissolve and the semi-coherent ones (indicated by ‘) begin to generate by nucleating on dislocations.

Then continued aging causes the equilibrium precipitation to occur.

Due to the incoherency of the new compound with matrix, its relatively large size and coarse distribution, mechanical properties reduce significantly [10].

Nevertheless the optimal condition to reach maximum hardness corresponds to about 90% of coherent and 10% of semi-coherent precipitates.

Finally, as for solution treatment also during ageing the control of temperature and time is essential. Otherwise the precipitates would be incoherent with matrix, too coarse and wouldn't induce great strengthening to the alloy [9,10].

### 1.3.1 Heat treatment of Al-Si-Cu-Mg and Al-Si-Mg alloys

The major phases in as-cast microstructure of Al-Si alloys are primary  $\alpha$ -Al, eutectic Si (whose morphology depends on the presence of chemical modifiers such as strontium) and intermetallic phases [7,8].

In chronological order during solidification the sequence of phase formation in hypoeutectic Al-Si-Cu-Mg alloys is [9,10]:

1.  $\text{Al}_{15}(\text{Mn, Fe})_3\text{Si}_2$
2.  $\alpha$ -aluminum phase,  $\text{Al}_{15}(\text{Mn, Fe})_3\text{Si}_2$  and/or  $\text{Al}_5\text{FeSi}$
3. Eutectic phase (Al+Si),  $\text{Al}_5\text{FeSi}$  and  $\text{Mg}_2\text{Si}$
4.  $\text{CuAl}_2$

Copper forms an intermetallic phase with Al that precipitates during solidification either as blocky  $\vartheta$ - $\text{CuAl}_2$  or as alternating lamellae of  $\alpha$ -Al +  $\text{CuAl}_2$ .

Otherwise during solidification copper can create other compounds in combination with magnesium and with different chemical compositions: ternary S- $\text{CuMgAl}_2$ , quaternary Q and  $\lambda$  phases (Q and  $\lambda$  consist of Al, Cu, Mg, Si and are characterised by the uncertainty in the stoichiometric composition, even more in precipitate form, which changes according to the chemical composition of the alloy) [11]; while in presence of iron generates other ones as  $\text{Cu}_2\text{FeAl}_7$ .

The  $\text{CuAl}_2$  phase can be blocky shape or finely dispersed  $\alpha$ -Al and  $\text{CuAl}_2$  particles within the inter-dendritic regions.

The presence of nucleation sites such as  $\text{Al}_5\text{FeSi}$  platelets or high cooling rates during solidification can result in fine  $\text{CuAl}_2$  particles. The blocky  $\text{CuAl}_2$  phase particles are difficult to dissolve during solution treatment, unlike the fine  $\text{CuAl}_2$  phase particles that can dissolve within 2 hrs.

Magnesium is usually present as  $Mg_2Si$  in Al-Si-Mg alloys if it's not in solution, but it can also form quaternary compounds with other alloy elements.

Moreover in absence of copper Fe and Mg can combine to produce  $\pi-Al_8FeMg_3Si_6$  (which is difficult to dissolve during solution treatment) [9,10].

- Solution treatment

In Al-Si-Cu-Mg alloys the aims of solution treatment are mainly the dissolution of Cu- and Mg- rich particles formed during solidification (that is  $CuAl_2$  and  $Mg_2Si$ ), homogenization of the as-cast microstructure and alloying elements and spheroidisation of eutectic Si particles.

These features impart improved ductility and fracture toughness to the component and reduce micro-segregation of other alloying elements in the primary Al matrix [9,10].

The time at the nominal solution treatment temperature must be long enough to homogenize the alloy and must then be chosen carefully to allow the maximum dissolution of intermetallic phases.

In alloys containing high levels of copper complete dissolution of  $CuAl_2$  phase is not usually possible.

The time needed for this stage depends on the as-cast microstructure (that is the size, distribution and type of intermetallic phases and the morphology of the Si particles) and on the temperature used.

The temperature that can be used is limited by incipient melting of phases formed from the last solidified melt, that is rich in solute elements due to segregation. Localised melting results in distortion and substantially reduced mechanical properties [9,10].

Cast Al-Si-Mg alloys can be solution treated at about 550 °C, while in Al-Si-Cu-Mg alloys having a low magnesium content (0.5% wt.) it's recommended to use a solution temperature of 495-500°C, because at 505°C fusion of copper-rich phases can occur.

Finally not all phases dissolve during a solution treatment.

In fact the Q phase is reported to be stable or to dissolve very slowly for alloys having a high Cu concentration (3.5-4.4% wt.) and various Mg concentrations when solution

treated at 500°C, while the  $\pi$ -Fe phase transforms into the  $\beta$ -Fe phase and Mg in solid solution when the Mg concentration is low (0.3-0.4% wt.) [9,10].

- Quench

The quench rate is especially critical in the temperature range between 450 °C and 200 °C for most Al-Si casting alloys, where precipitates form rapidly due to a high level of supersaturation and a high diffusion rate.

At higher temperatures the supersaturation is too low, while at lower ones the diffusion rate is too low for precipitation to be critical [9,10].

For example in Al-Si casting alloys silicon may diffuse from the matrix to eutectic Si particles and  $Mg_2Si$  phases may form on the eutectic Si particles or in the matrix, reducing the supersaturation of magnesium and silicon in the matrix [10].

Moreover the effectiveness of the quench is dependent upon the quench media (which controls the process rate) and interval.

The media used for quenching aluminium alloys include water, brine solution and polymer solution. Water is usually the dominant quenchant for aluminum alloys, but it often causes distortion, cracking and residual stress problems [10].

Considering Al-Si-Mg alloys, if water at 25°C is used as a quenchant the  $\alpha$ -Al matrix consists of a large number of needle-shaped and coherent  $\beta''$ - $Mg_2Si$  precipitates [10].

The size of the precipitates is approximately 3 to 4 nm in diameter and 10 to 20 in length. Instead with a water quench at 60°C the density of the precipitates decreases, while their size increases slightly; at the same time a significant number of fine Si precipitates resulting from precipitation of excess silicon could be observed in the  $\alpha$ -Al matrix.

Otherwise with a slow quench in air, very different precipitation features are normally evidenced. In fact the material remains at high temperatures for a longer period, which enhances the diffusion of silicon and magnesium.

So besides a high density of fine  $\beta''$ - $Mg_2Si$  precipitates the  $\alpha$ -Al matrix also contained a large number of areas with coarse rods  $\beta'$ - $Mg_2Si$  grouped parallel to each other [10].

- Ageing

The age hardening response depends on the fraction, size, distribution and coherency of precipitates formed. Al-Si-Cu-Mg alloys and Al-Si-Mg alloys generally have a high age hardening response, while Al-Si-Cu alloys have a slow and low one [9].

The main process of precipitation in Al-Si-Cu, Al-Si-Mg and Al-Si-Cu-Mg alloys can be summarized as follows: supersaturated solid solution; formation of GP zones; formation of metastable phases; formation of equilibrium phases [10].

In particular the precipitation sequence for an Al-Si-Cu alloy is based upon the formation of  $\text{CuAl}_2$ -based precipitates.

The precipitation sequence of this phase develops generally as follows [10]:



The sequence begins with the clustering of Cu atoms, which then leads to the formation of coherent, disk-shaped GP zones.

During ageing GP zones arise homogeneously; these zones manifest as two-dimensional, copper-rich disks.

As time increases, these GP zones increase in number while remaining approximately constant in size.

As the ageing temperature is increased above 100°C, the GP zones dissolve and are replaced by  $\theta''$  precipitates. These precipitates are three dimensional disk-shaped plates having an ordered tetragonal arrangement of Al and Cu atoms;  $\theta''$  also appears to nucleate uniformly in the matrix and is coherent with the matrix in binary Al-Si-Cu alloys.

The high degree of coherency gives great strengthening to the material. As aging proceeds, the  $\theta''$  starts to dissolve and  $\theta'$  begins to form by nucleating on dislocations.

The latter also has a plate-like shape and is composed of Al and Cu atoms in an ordered tetragonal structure, but, as it grows, loses coherency with the matrix and so a decrease in strength properties may be observed, while continued aging causes the equilibrium  $\theta$ - $\text{CuAl}_2$  precipitate to occur.

Tetragonal in shape, the  $\theta$  phase is completely incoherent with the matrix. Due to its morphology, its relatively large size and coarse distribution, mechanical properties reduce significantly [10].

Instead the sequence of precipitation in Al-Si-Mg alloys can be described as follows [10]:

- i. Precipitation of GP zones
- ii. Intermediate phase  $\beta''$ -Mg<sub>2</sub>Si
- iii. Intermetallic phase  $\beta'$ -Mg<sub>2</sub>Si
- iv. Equilibrium phase  $\beta$ -Mg<sub>2</sub>Si, FCC structure, rod or plate-shaped.

The maximum alloy strength (peak-aging) is achieved just before the precipitation of the incoherent  $\beta$ -platelets.

Thus during ageing the dissolution of unstable clusters increase the solute concentration, while larger clusters that are stable remove solute by growing into GP zones that become nucleation sites for  $\beta''$  [9].

The precipitation sequence for Al-Si-Cu-Mg alloys is similar but more complex, as  $Q''$ ,  $S''$ ,  $\lambda''$  and  $\theta''$  phase may also form.

The precipitation sequence in copper-containing alloys is influenced by the high density of dislocations formed during quenching due to the difference in thermal expansion between the Si particles and the  $\alpha$ -Al matrix.

For example fine and evenly dispersed  $\theta''$  phases form in the centre of the dendrites, while coarse  $\theta'$  phases form on the dislocations, close to the Si particles.

The semi-coherent phases have a negligible strength contribution and can be seen as a loss of Cu and Mg atoms, that could have increased the fraction of coherent precipitates [9,10].

#### **1.4 Thermal stability of precipitates**

Alloying elements such as copper and magnesium are often added to improve alloy strength at room temperature as well as at higher temperatures.

Nevertheless these elements generate compounds (such as CuAl<sub>2</sub>, Mg<sub>2</sub>Si and CuMgAl<sub>2</sub>), which can only be effective for strength and creep resistance at temperatures below 200-

250°C, in fact above 250°C they tend to become unstable, coarsen rapidly (due to Ostwald ripening) and then dissolve, leading to an alloy with an undesirable microstructure for high temperature applications.

Therefore the behaviour of magnesium and copper compounds at high temperature forces the addition of other alloying elements, that are able to generate intermetallics and/or precipitates with elevated thermal stability, by which increase the alloys' one [12].

### 1.4.1 Change of composition for high temperature applications

To improve the alloy performances under these conditions, the presence of thermally stable and coarsening-resistant compounds is required and so other alloying elements have been considered.

The most commonly employed ones are as follows:

- **Nickel** – Nickel demonstrates low diffusivity and solid solubility and is able to change the morphology of iron intermetallics and increase high temperature performances by creating thermally stable compounds. Otherwise the presence of this element alone is negative: reduces ductility, toughness and mechanical resistance of alloys [13].

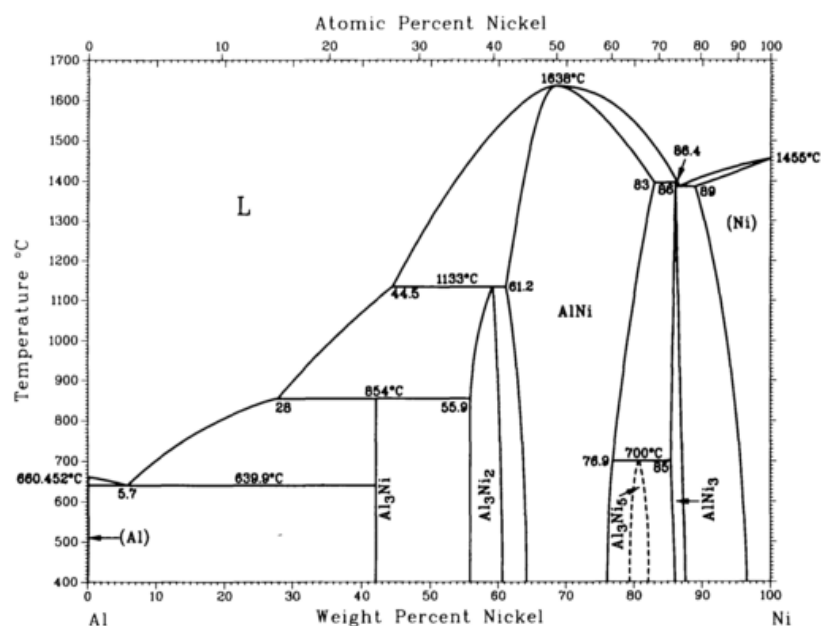
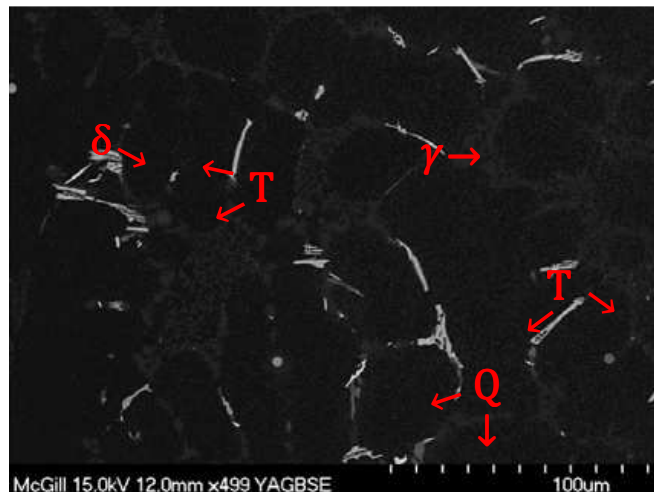


Figure 6 – Aluminum-nickel phase diagram [14]

For example the addition of 0.4% wt. in nickel causes a decrease in tensile properties of about 10% compared with the base alloy, that is attributed to the formation of brittle compounds and to a Ni–Cu reaction which interferes with the formation of  $\text{CuAl}_2$  precipitates, thereby affecting the age hardening process [15]. But in combination with zirconium not only nickel's detrimental effects can be counterbalanced but also high temperature properties are able to further improve. It may be deduced that the elements must interact between themselves or with other elements contained in the base alloy in order to form new phases, which partially reduce the quantity of element free to generate brittle intermetallics and enhance mechanical performances of alloys (both at room and at high temperatures) [15].

In particular an alloy containing 0.2% wt. in Zr + 0.2% wt. in Ni exhibits the highest increase of mechanical properties at room and high temperatures: ultimate tensile and yield strength at room temperature are respectively 7% and 9% higher than that of base alloy, while at 300°C they are 70% and 39% bigger [16].



**Figure 7 - Microstructure of the as-cast alloy containing nickel. T, Q,  $\gamma$  and  $\delta$  phases can be distinguished [13]**

Otherwise the negative effects of nickel compounds can be partially reduced by adding traces of manganese. In fact the latter dissolves in some intermetallics (especially  $\text{T-Al}_9\text{FeNi}$ ), increasing their ductility and then also that of alloy; otherwise manganese doesn't enhance significantly the mechanical performances, because in presence of iron creates  $\alpha\text{-Al}_{15}(\text{Fe}, \text{Mn})_3\text{Si}_2$ , that is brittle too.

The beneficial effects of nickel can be improved by applying heat treatment, guaranteeing an enhancement in mechanical performances. In fact some brittle compounds as  $\delta\text{-Al}_3\text{CuNi}$  and  $\gamma\text{-Al}_7\text{Cu}_4\text{Ni}$  tend to dissolve during solution treatment and during ageing are “replaced” by  $\vartheta\text{-CuAl}_2$  and  $\text{Q-Al}_5\text{Mg}_8\text{Cu}_2\text{Si}_6$ , which reduce embrittlement and increase resistance [11].

Finally at elevated percentages (1% wt.) nickel even reduces creep resistance, quickening the phenomenon and in addition to disadvantages reported before its elevated cost and density ( $\approx 8.9 \text{ g/cm}^3$ ) limit further the utilization of this alloying element [16].

- **Zirconium** – Zirconium is suitable as alloying element thanks to its low diffusivity, solid solubility and the capability of creating reinforce phases.

It's capable of increasing mechanical resistance, hardness, wear resistance (both at room and high temperature) and overall thermal stability.

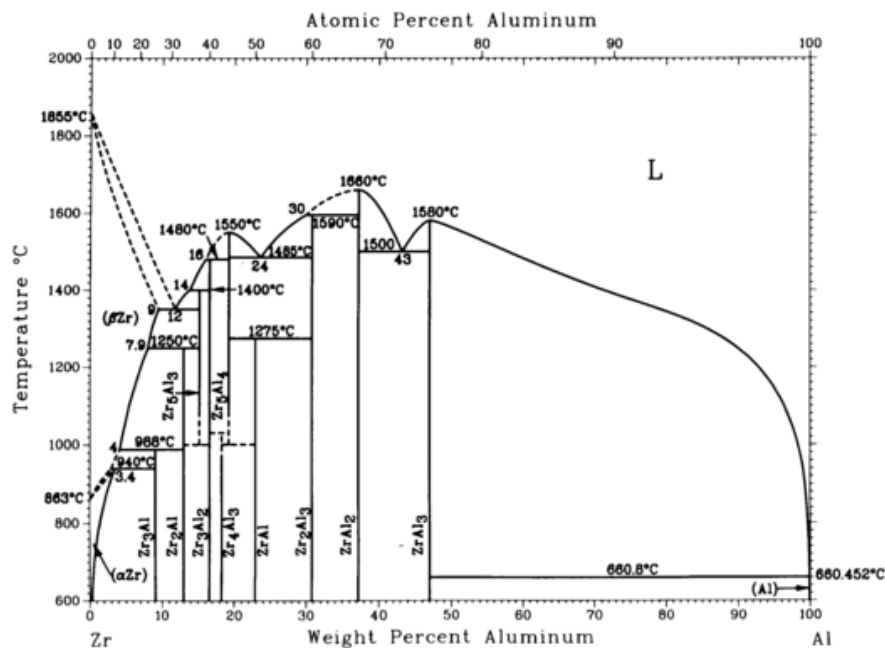


Figure 8 – Aluminum-zirconium phase diagram [17]

Inside Al-Si-Cu-Mg alloys it's usually employed below  $\sim 0.15\%$  wt., in order to avoid the primary precipitation of the peritectic trialuminide  $\text{Al}_3\text{Zr}$ , which exhibits a peritectic phase equilibrium with the terminal  $\alpha\text{-Al}$  solid solution [18].

This solute-rich primary compounds is the first solid to form under equilibrium conditions and grows into coarse phase during conventional casting, leaving the remaining melt, and ultimately the solidified  $\alpha$ -Al solid solution, substantially depleted in solute.

This would decrease the amount of solute retained in solid solution and therefore would limit the potential for precipitation strengthening during ageing.

Moreover the formation of this phase during solidification results in a progressive refinement of the as-cast grain structure and this would affect the creep resistance of the alloy.

Zirconium is often employed in combination with other alloying elements to improve the performances: for example in addition to nickel (read “Nickel” subchapter above) or with titanium and vanadium.

There are discordant theories about the optimal percentages of zirconium, titanium and vanadium to utilize, in fact in literature 0.06-0.2%, 0.02-0.2% and 0.1-0.2% (wt.) are reported [18,19,20].

Additions of zirconium, vanadium and titanium resulted in the formation of many Zr-V-Ti-rich phases, which are often observed in the form of agglomerates adjacent to each other, indicating that they could nucleate simultaneously during solidification process.

After solution treatment they remain in the microstructure, because just partial dissolution of them occurs and so this indicates that some concentrations of Zr, V and Ti were available for the subsequent precipitation process (Ti and V additions increase the effective supersaturation of Zr), during which  $Al_3(Zr, V, Ti)$  (as mixed or single-element aluminide) precipitate.

These compounds exhibit reduced coarsening compared to the binary  $Al_3Zr$  phase. This in return results in improved precipitates' stability and consequently better ability to retain their coherency with the metal matrix at elevated temperatures [21].

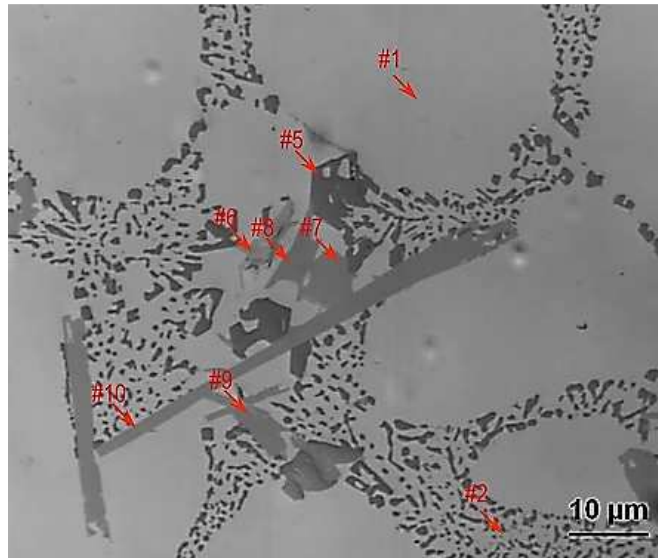


Figure 9 – Optical microscope image representing microstructure of as-cast Al–Si–Cu–Mg alloy modified with Ti, V and Zr. Several phases can be distinguished:  $\alpha$ -Al dendrites (#1), Al-Si eutectic (#2),  $\theta$  -  $\text{CuAl}_2$  (#3),  $\text{Al}_2\text{CuSi}$  ternary eutectic (#4), Q phase (#5),  $\pi$ - $\text{Al}_8\text{FeMg}_3\text{Si}_6$  (#6),  $(\text{AlSi})_3(\text{VZr})$  (#7),  $(\text{AlSi})_2(\text{TiZr})\text{Fe}$  (#8),  $(\text{AlSi})_3(\text{TiVZr})$  (#9) and  $(\text{AlSi})_3(\text{TiZr})$  (#10) [21]

An exception was reported by S.K. Shaha et al., who added 0.21% Ti-0.30% V-0.47% Zr (wt.) to Al–7Si–1Cu– 0.5Mg–0.1Ti cast alloy.

This formulation led to the formation of  $(\text{AlSi})_x(\text{TiVZr})$  phases with increased thermal stability during solidification, which are stable up to 700°C. Although the zirconium content in the investigated alloy was above the peritectic concentration of 0.15%, the properitectic primary  $\text{Al}_3\text{Zr}$  phase did not form as a stand-alone structure due to dissolution of  $\text{Al}_3\text{Ti}$  and  $\text{Al}_3\text{V}$  in  $\text{Al}_3\text{Zr}$  [21].

As reported before there are discordant ideas about the optimal amount for every alloying element and this substantial variability reported in literature makes necessary to go on searching for the ideal percentages.

- **Vanadium** - Its presence inside the alloy improves mechanical properties and its beneficial effect can be further enhanced by heat treatment (the improvement is greater than that obtained for nickel-containing alloys).

Nevertheless the reinforce mechanism hasn't been still completely understood (maybe like other alligants it dissolves inside some intermetallics, increasing their ductility).

It's reported its use in percentages between 0.02 - 0.2 % wt., often in combination with zirconium and titanium, resulting in the formation of thermally stable compounds (read subchapter about zirconium) [15, 16].

- **Molybdenum** – It's characterised by low diffusivity and solid solubility (which are some of the features requested to alloying elements), modifies iron intermetallics morphology from a plate-like to a blocky phase and creates  $\alpha$ -Al-(Fe, Mo)-Si, a compound coherent with matrix which develop during solution treatment, thermally stable (they retain their strengthening effect at 300°C) and concentrate in inter-dendritic areas [22, 23].

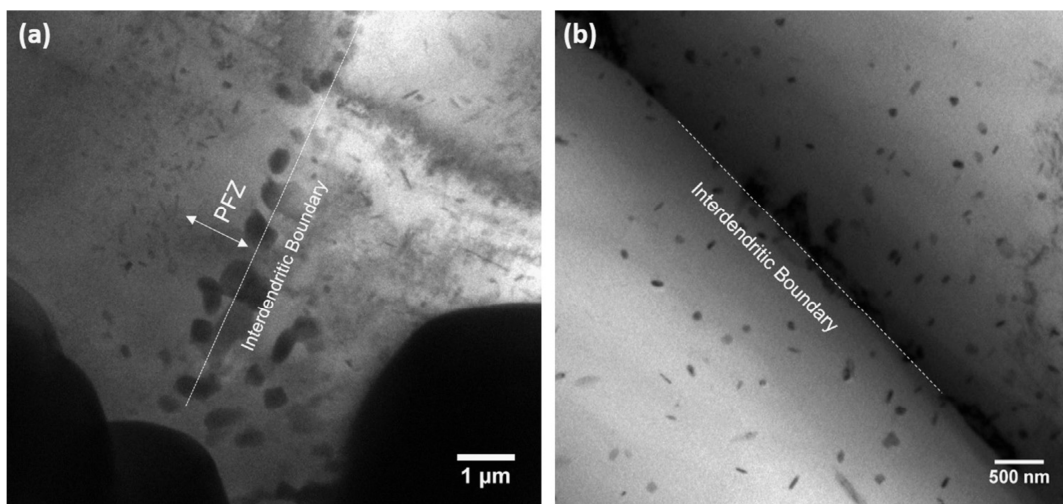


**Figure 10 – Images of  $\alpha$ -Al-(Fe, Mo)-Si phase distribution in inter-dendritic regions of the alloy after solution treatment [22]**

Thanks to the fine phase created the dislocation motions are effectively hindered and consequently the modified alloy exhibits significant improvement in the creep properties and mechanical resistance at high temperature, reaching the best results at 0.3% wt.: at 300°C and 30 MPa the minimum creep rate decreases ~95% and the creep time-to-fracture increases from 50 min to 1500 min compared to the base alloy.

Instead yield strength, ultimate tensile strength and elongation at 300°C of the Mo-containing alloy were increased by ~25, 15 and 35% respectively compared to the base alloy [22].

Moreover in combination with Mn the results may even improve. In fact increasing Mn content up to 0.5% increases the number of dispersoids per unit area, while their average size decreases, resulting in an enhancement of creep

resistance (at 300°C and 30 MPa minimum creep rate decreases and creep time-to-fracture increases to 180h) [23].

### **1.5 Aim of the research**

The aim of the research has consisted of the use of molybdenum (so far not much considered) as alloying element for A354 alloy, the definition of the optimal quantity, the study of its potentiality as such and the possible synergetic action in addition to other elements.

Moreover great attention was set on the possibility of applying a heat treatment (trying also to improve process parameters) to enhance alloy performance.

## Chapter 2 – Material and methods

### 2.1 Material

As previously reported the aluminium alloy analysed during this study was the A354, an Al-Si-Cu-Mg alloy whose specific composition is described in table 2.1:

%Al	%Si	%Cu	%Mg	%Fe	%Mn	%Ti
bal.	8.44-8.70	1.69-1.79	0.45-0.48	0.11-0.12	0.003-0.004	0.120-0.123

Table 2.1 – Nominal chemical composition of A354 alloy (wt%.)

Subsequently, in order to modify base alloy and reach the desired composition and microstructure, the addition of a modifier (strontium) and an alloying element (molybdenum) was provided through the use of master alloys (Tables 2.2 and 2.3).

%Al	%Sr	%Si	%Mg	%Fe	%Mn
bal.	9.5	0.03	0.07	0.25	0.01

Table 2.2 – Nominal chemical composition of strontium master alloy (wt%.)

%Al	%Mo	%Si	%Mg	%Fe	%Mn
bal.	9.7	0.16	0.01	0.08	0.01

Table 2.3 – Nominal chemical composition of molybdenum master alloy (wt%.)

In particular 300ppm of strontium and different amount of Mo (0.1, 0.3, 0.5 and 0.8 wt%) were added in the alloy, in order to analyse and compare their effect on mechanical properties.

### 2.2 Mould preparation

The mould used for casting permitted to obtain 5 cylindrical rods at the same time (Fig.2.1): the external and central rods were approximately 12 cm in length and 1.5 cm in diameter, while the bigger ones (which were the sprues) respectively 12 and 5 cm.

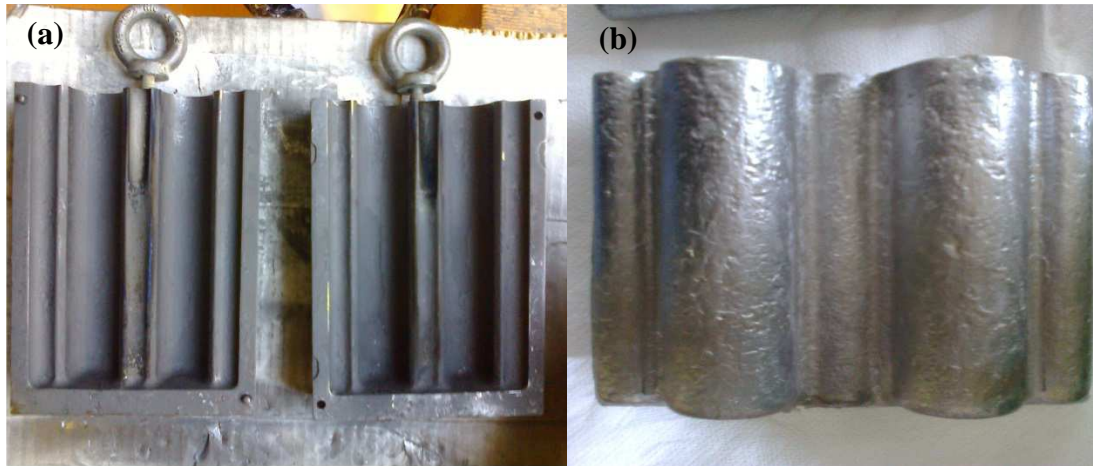


Figure 2.1 – Mould employed for casting (a) and cast obtained (b)

To limit its wear and avoid the migration of iron in the alloy (which is undesirable, because it would create brittle and needle-like intermetallics) a solution with graphite was sprayed on the internal surface of every semi-mould, also facilitating detach of material after casting.

The mould was pre-heated at 200°, before every casting, in order to avoid the premature solidification of molten metal during casting, which would hinder mould filling.

### 2.3 Casting

The alloys were produced by gravity die casting using “Topcast Engineering TVCs” vacuum casting machine.

Melting is achieved in protective atmosphere (Argon), while a vacuum pump is provided in order to boost the suction effect into the mould.

Graphite melting pot consumption is greatly reduced thanks to the “gaswash” procedure, which removes the oxygen in few seconds from the charge loading operation. The machine is fully automatic making the operator’s job very easy and less dangerous. Moreover the presence of magnetic stirring permits a better mixing and the reduction of inhomogeneities (otherwise this would occur due to different density of aluminium and its alloying elements).

The commercial A354 alloy has been provided in form of ingots, which were cut in small pieces and then melted in a resistance furnace, set at 800 °C, in a standard clay-graphite crucible and every cast was about 1 kg in weight.

In each cast the addition of strontium was provided, in order to get the modification of eutectic Si, which turns its acicular morphology into a spherical one, eliminating its embrittling effect.

With respect to A354 alloy the optimal amount of Sr to get a completely modified microstructure has already been discussed in a previous study and was equal to 300 ppm (that is 3 g for 1 kg cast) [24, 25].

Moreover, before their addition, modifiers and alloying elements (in form of master alloy) were pre-heated for about ten seconds to eliminate the moisture.

In fact, due to the high temperature, water would decompose in hydrogen and oxygen, creating a flammable mixture (that would be activated by high temperature itself).

Subsequently, after its complete melting, aluminium was maintained at 800°C for 10 minutes under magnetic stirring in Argon atmosphere, in order to get the whole cast homogeneity (casting sequence A).

This particular aspect was considered after the identification of inhomogeneities and clusters of intermetallics in some preliminary castings containing 0.3%wt of molybdenum.

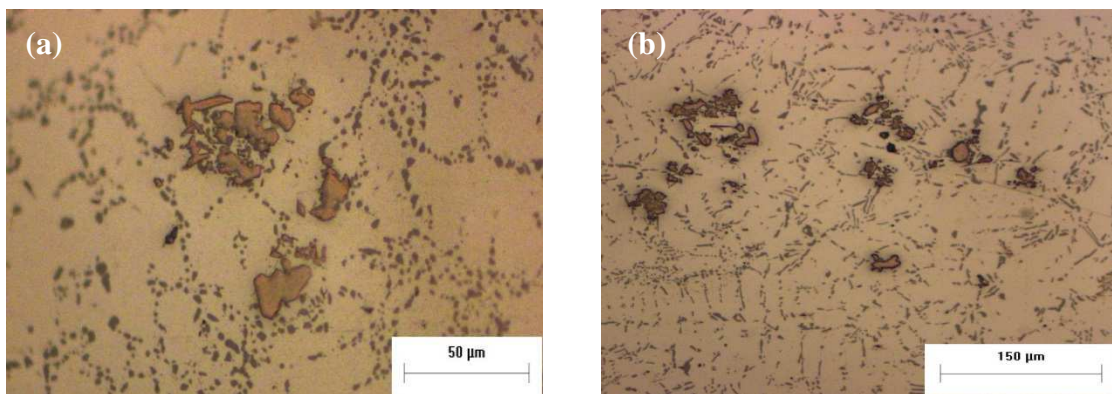


**Figure 2.2 - Optical micrographs of A354 containing molybdenum casted after keeping molten metal at 800°C for 10 min (casting sequence A)**

Despite this, inhomogeneities and molybdenum phase of great dimension (which appeared fairly identical to that present into the correspondent master alloy) were still observed inside casts. For this reason the melting sequence was modified: after complete melting at 800°C temperature was raised up to 900°C (at which molten metal was

maintained for 20 minutes), then was lowered to 800°C (maintained for 10 minutes) and finally casting was carried out (casting sequence B).

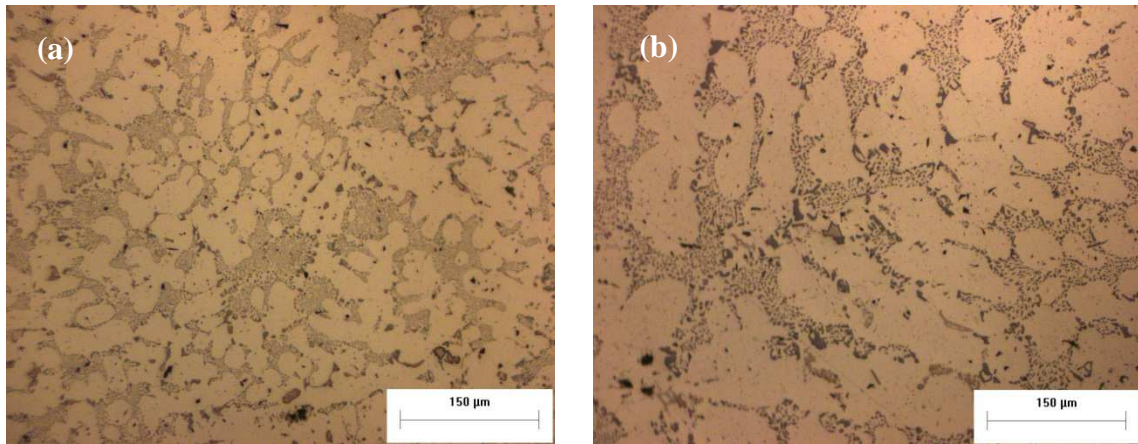


**Figure 2.3 - Optical micrographs of A354 containing molybdenum casted after keeping molten metal at 800°C for 10 min + 900°C for 20 min (casting sequence B)**

Higher temperature and longer time of process increased dissolution of molybdenum compounds and its diffusion, improving the homogeneity of cast.

Then, after casting, the hot material was extracted from mould, to facilitate the procedure, and immediately quenched in water.

Finally, after cast cooling, a band saw was used to separate each rod from the others, then the sidebars were machined to obtain specimens.

## 2.4 Chemical analysis

Chemical analysis of a cast sample was performed with Glow Discharge-Optical Emission Spectroscopy (GD-OES) technique to define its real composition.

GD-OES is a fast, low-cost and easy-to-use analytical technique, which can provide rapid and simultaneous analysis of all elements of interest inside solids (metals, powders, polymers, glasses and ceramics).

Two types of analyses can be performed:

1. bulk analysis: global chemical analysis
2. depth profiling analysis: signal from each chemical element as a function of erosion time

Bulk analysis can be performed in less than one minute. Moreover the technique has the added capability of direct depth profiling of the solid sample without the need for any prior preparation.

An uninterrupted quantitative depth profile analysis by GD-OES takes only minutes and provides a complete detailed sample-composition map at depths ranging from less than 10 nanometres to more than 100 micrometres.

However the samples underwent only bulk analysis.

On each sample (previously smoothed and polished) three valid measures were performed and the average values were calculated: the chemical compositions were coherent with the hypothesized ones for a Mo addition between 0.1 and 0.3%, while, for higher Mo addition, the percentage revealed by chemical analysis was different from the theoretical one.

This may be due to cast inhomogeneity and presence of clusters of molybdenum-based intermetallics, which interfered with measurements.

## **2.5 Heat treatment**

After casting the specimens were subjected to T6 heat treatment, in order to increase their mechanical properties.

Three different heat treatments were considered:

1. Solution treatment (495°C for 6h + 515°C for 2h) + quenching (water at 60°C) + ageing (180°C for 4h)
2. Solution treatment (495°C for 6h + 540°C for 1h) + quenching (water at 60°C) + ageing (180°C for 4h)
3. Solution treatment (495°C for 6h + 540°C for 10h) + quenching (water at 60°C) + ageing (180°C for 4h)

The first one was optimized in a previous work developed at the School of Engineering of Bologna University, according also to results of [24, 25]; while the second and the third ones were reported in an article written by Farkoosh et al. [22].

Specifically the higher temperature of solubilisation (that is 540°C) is justified by the development of molybdenum dispersoids, thermostable nanometric compounds able to increase high temperature and creep resistance [22].

After every phase of heat treatment a sample coming from every alloy was taken out of the oven and employed for hardness measures, in order to evaluate the effects of heat treatment steps on hardness.

After first analysis it was clear that alloys containing molybdenum subjected to 540°C solution treatment could reach higher performances compared to that undergone to the 515°C one.

Moreover, due to interesting results already obtained after solution treatment at 540°C and, in order to verify if it would be possible to avoid quench and ageing phases, obtaining technologic advantages and cost savings, it was established to analyse and compare the performances of alloys subjected to:

1. Solution treatment (495°C for 6h + 540°C for 1h) + air cooling
2. Solution treatment (495°C for 6h + 540°C for 1h) + quench (water at 60°C)
3. Solution treatment (495°C for 6h + 540°C for 1h) + quench (water at 60°C) + ageing (180°C for 4h)
4. Solution treatment (495°C for 6h + 540°C for 10h) + air cooling
5. Solution treatment (495°C for 6h + 540°C for 10h) + quench (water at 60°C)
6. Solution treatment (495°C for 6h + 540°C for 10h) + quench (water at 60°C) + ageing (180°C for 4h)

After heat treatment a samples were subjected to high temperature exposure, in order to assess their mechanical behaviour after high temperature soaking (Table A.1 in Appendix) drawing hardness vs high exposure duration curves (degradation curves).

Due to results of hardness obtained by alloys solubilised at 515°C, the study concentrated only on the ones treated at 540°C (see chapter “3.5.1”).

In the specific, to define the optimal solubilisation time at 540°C and have a comparison term with a similar diagram reported by Farkoosh et al. [22], it was determined the hardness trend over solubilisation time.

A set of samples containing 0.3% in Mo was submitted to the first phase of heat treatment (at 495°C for 6h), after that each one was solubilized at 540°C for a specific time, then a half was air cooled, while the other half was quenched in water at 60°C. Finally a series of hardness measures was carried out at specific intervals.

## **2.6 High temperature exposure**

Before machining samples of A354 alloy and all Mo-containing alloys were soaked at high temperatures, in order to simulate the over-aging of the material during high temperature exposure, obtaining hardness vs high exposure duration curves.

As a consequence of the previous hardness results, it was established to evaluate performances of samples after air cooling, quench and quench + ageing.

Specifically two different temperatures were chosen, in order to test the response of analysed materials:

1. 245°C (average temperature in cars engines)
2. 300°C (maximum reachable temperature in engines)

In particular during tests the first one was prolonged up to 301h (for samples solubilised at 540°C for 1h) and 144h (for the ones solution treated at 540°C for 10h), in order to confirm the gap in hardness measurement observed by Farkoosh between base alloy and modified one after some weeks of degradation [22]; while the temperature of the second series of measures was increased to 300°C, so as to analyse exclusively the reinforcement inducted by molybdenum-containing phases, which can't be modified at this temperature unlike copper precipitates, that above 250°C undergo Ostwald ripening and dissolution [22].

On each sample three valid hardness measures were performed and the average values were calculated, then they were utilised to draw over-ageing curves.

## **2.7 Hardness measurement**

According to the technological concept the hardness is defined as the resistance opposed to penetration by a material surface.

Even if the hardness value itself isn't sufficient to judge a material, this technique is cheap, rapid, not destructive and gives interesting information.

The tests work on the basic premise of measuring the critical dimensions of an indentation left by a specifically dimensioned and loaded indenter.

Hardness measurements have been carried according to standards HB<sub>10</sub> and HV<sub>0.1</sub> and the values respectively obtained using the following relationships:

$$HB_{10} = \frac{2F}{\pi D (D - \sqrt{D^2 - d^2})} \qquad HV_{0.1} = 1.854 * \frac{F}{d^2}$$

On solubilized specimens 3 macro-hardness Brinell and 5 micro-hardness Vickers (just on  $\alpha$ -phase) measures were performed, while on aged and degraded ones only Brinell measures were made.

Before Brinell hardness tests samples surfaces were smoothed with SiC grinding papers, used in decreasing grain size order (180-320-400-600-800 grit).

Measurements were carried out using a GALILEO A200 durometer with 2.5 mm diameter indenter and applying 62.5 kg of load. Indentation were then photographed with a ®ZEISS AX10 optical microscope and after that the image analyser software ®IMAGE PRO-PLUS was used to measure their diameter (the measure was repeated twice for any diameter, in order to minimize the possible error induced by the not perfect circularity of the mark); the average values for each sample were calculated.

Micro-hardness Vickers measures the samples were smoothed with grinding papers and subsequently polished with an automatical lapping machine, using 2 diamond powder suspensions of 9 and 3  $\mu$ m.

The measurements were performed with a GALILEO micro-durometer, with 0.098 kg load.

The hardness was measured directly with the same instrument: the average value over five measurements for each sample was calculated

Vickers measurements were performed for evaluating primary  $\alpha$ -Al phase hardness: however the samples analysed were characterised by a fine microstructure and therefore it isn't possible to guarantee that the values weren't affected by the contribution of harder eutectic silicon and intermetallics.

## 2.8 Metallographic analysis

The metallographic analysis allows the observation and the study of alloys microstructure.

In order to perform microstructural characterisation, samples surfaces were smoothed with SiC grinding papers, used in decreasing grain size order (200-320-400-600-800-1200-2000 grit) and then polished on 4 cotton clothes set on an automatic lapping machine, on which respectively 3 diamond powder suspensions of 9, 3 and 1  $\mu\text{m}$  and a silica one of about 0.5  $\mu\text{m}$  were spread.

Every sample had to be washed with water after every step on sandpapers and clothes, so that it was possible to remove every residue (SiC from grinding papers, fibers from clothes, aluminum from samples themselves), which would contaminate the metallographic specimens.

At the end of polishing phase instead the specimens were washed with water, then acetone and after that dried with cold air, so that rings (which would disturb the subsequent micrographic analysis) couldn't appear.

Then the samples were analysed through optical (@ZEISS AX10) and scanning electron microscopy (@ZEISS Evo 50), provided of Energy Dispersive Spectrometer (EDS).

Thanks to the different magnifications it was possible to study the microstructure of the alloys and in particular the different compounds developed during solidification.

The presence of intermetallics, in fact, is important, because they influence material properties such as mechanical and corrosion resistance.

Their identification is possible thanks to their different morphology and colour (or brightness) and through Energy Dispersive Spectrometer (EDS).

Unluckily, due to nanometric dimension of molybdenum dispersoids (generated during solution treatment at 540°C), it wasn't possible to observe and analyse them by using SEM (and obviously neither by optical microscope).

## **2.9 Secondary Dendrite Arm Spacing (SDAS) measurement**

The Secondary Dendrite Arm Spacing is the distance between the secondary arms of dendrites forming the alloy.

Measures were carried out on low magnification micrographs (magnification 2.5X) and at least 7-8 SDAS values were measured, by using @IMAGE PRO-PLUS software.

## **2.10 Thermal analysis**

The term “thermal analysis” stands for a group of techniques, in which a physical property of a material is measured as a function of temperature, while it's subjected to a controlled temperature programme.

DSC allows the study of transitions and transformations, which occur in materials, by measuring the difference in heat absorbed or released by sample (associated with material transitions) compared to inert reference as a function of temperature.

The analysis was conducted on a sample of A354 + 0.3% Mo alloy with the purpose of determining the development of molybdenum dispersoids (as reported by Farkoosh) and other phases present in the alloys.

Specifically the analysis was conducted in inert atmosphere (argon flux = 30 mL/min) with a set heating ramp from room temperature up to 700°C (over the reach of complete melt) with a rate of 20°C/min.

## **2.11 Tension tests**

Mechanical testing plays an important role in evaluating fundamental properties of materials as well as in developing new materials and in controlling their quality.

The most common test used to measure the mechanical properties of a material is the tension test.

Both room and elevated temperature (250 °C) tensile tests were performed, using a servo-hydraulic testing machine according to ISO standards: the first ones were carried out in agreement with the standard ISO 6892-1:2009, while the second ones followed the standard ISO 6892-2:2011.

Samples were obtained by side and central bars of casts (see fig.2.1) and were machined to obtain round dog-bone tensile specimens, characterised by gauge length=25 mm and gauge diameter=5 mm.

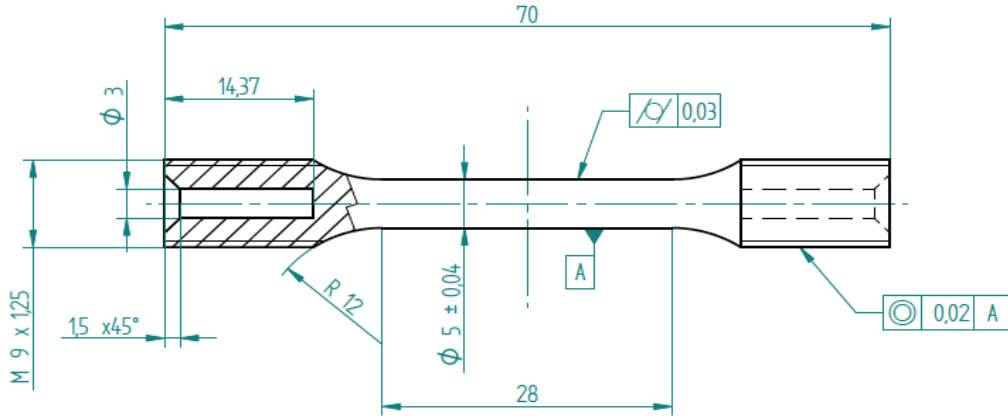


Figure 2.4 - Tensile test sample geometry

Just a preliminary study was conducted and then only three samples were tested in each working condition to obtain an average value. Further tests will be carried out subsequently.

The specimens employed for tension tests and corresponding heat treatment which underwent are reported in table 2.4.

Samples designation	Mo wt%	Treatment undergone	Test conditions
A T6	/	Solution treatment (495°C 6h + 540°C 1h) + quench + ageing (180°C 6h)	Room temperature
A OA	/	Solution treatment (495°C 6h + 540°C 1h) + quench + ageing (180°C 6h) + over-ageing at 250°C for 100h	250°C
MoA T6	0.3	Solution treatment (495°C 6h + 540°C 1h) + air cooling + ageing (180°C 6h)	Room temperature
MoA OA	0.3	Solution treatment (495°C 6h + 540°C 1h) + air cooling + ageing (180°C 6h) + over-ageing at 250°C for 100h	250°C
MoT T6	0.3	Solution treatment (495°C 6h + 540°C 1h) + quench + ageing (180°C 6h)	Room temperature
MoT OA	0.3	Solution treatment (495°C 6h + 540°C 1h) + quench + ageing (180°C 6h) + over-ageing at 250°C for 100h	250°C

Table 2.4 – Schematisation of tension samples, molybdenum content, corresponding treatment undergone before tests and test conditions

No tests were carried out on A354 samples at room temperature, because the specific data were already available.

## **2.12 Fractography**

Fractography is the study of fracture surfaces of materials.

The aim of the analysis is the evaluation of the failure mechanisms, by studying the morphology of a fractured surface.

The fracture surface analysis was performed with a Scanning Electron Microscopy ®ZEISS Evo 50, provided of Energy Dispersive Spectrometer (EDS).

A fracture surface was observed to analyse breaking mechanism and identify the composition of different phases (recognised with EDS).

# Chapter 3 - Results

## 3.1 Thermal analysis

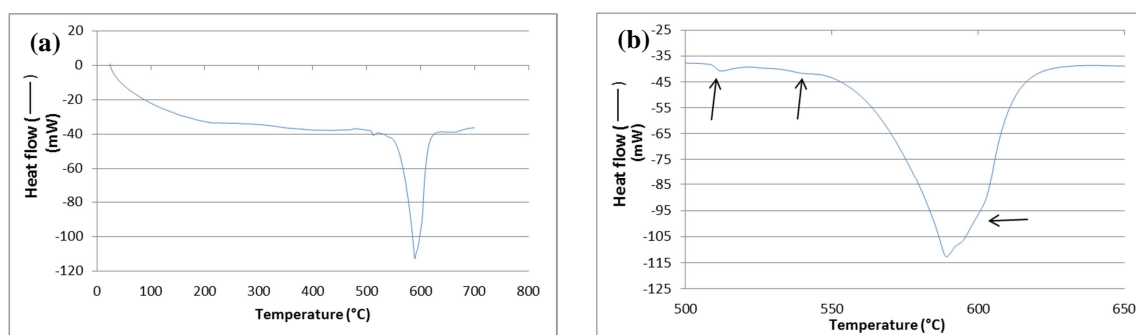


**Figure 3.1 – DSC analysis diagram of an A354+0.3%Mo sample. (a) reports the complete analysis and (b) a detail in which transitions (highlighted by the arrows) take place**

In graphs resulting from analysis it's possible to distinguish 3 different transitions: the first one related to melting of Cu-based intermetallics at about 512°C, the second one associated to that of Si-containing phases (at about 540°C), while the last one corresponding to complete melting of tested material (~589°C) and to which is associated the greatest enthalpy.

During the analysis it wasn't possible to determine any transition related to molybdenum dispersoids formation, which would have been developed at about 540°C.

It can be supposed that corresponding peak wasn't characterised by high transformation enthalpy and then was partially hidden by second transition.

## 3.2 Heat treatment

The data are reported considering “as cast” at time = 0, solution treatment at 495°C the range t=0-6h.

Therefore, for example, samples solubilized for 1h at 540°C correspond to data reported at 7h into the curves.

As a result of hardness measures carried out on air cooled and quenched samples, it was possible to build ageing curves (the corresponding data are reported in “Tables A.2 and A.3” in section “Appendix”):

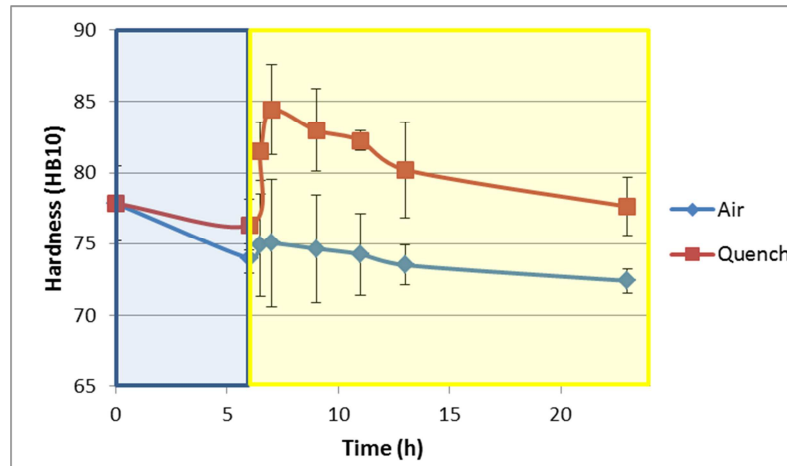


Figure 3.2 – Ageing curves at 540°C of quenched (red line) and air cooled (blue line) A354+0.3%Mo. Blue region corresponds to solution treatment at 495°C, while yellow one to ageing treatment at 540°C

The trend shows an increase resulting from the development of molybdenum dispersoids (which generated maintaining the alloy at high temperature) and reaches a maximum after about 1 hour of treatment both for air cooled and quenched samples.

Instead the subsequent decline in macrohardness after prolonged solution treatment is attributed to the coarsening of the dispersoids.

Moreover a further and substantial increase in hardness values was generated by quench itself. In fact a gap of fairly 10 HB between the two curves was recorded. This aspect was not considered in the study and could be related to the different strengthening precipitates (both Cu, Mg or Mo-based) that forms during quenching and air cooling.

### 3.3 Metallographic analysis

#### 3.3.1 Optical microscopy

##### 3.3.1.1 A354 alloy

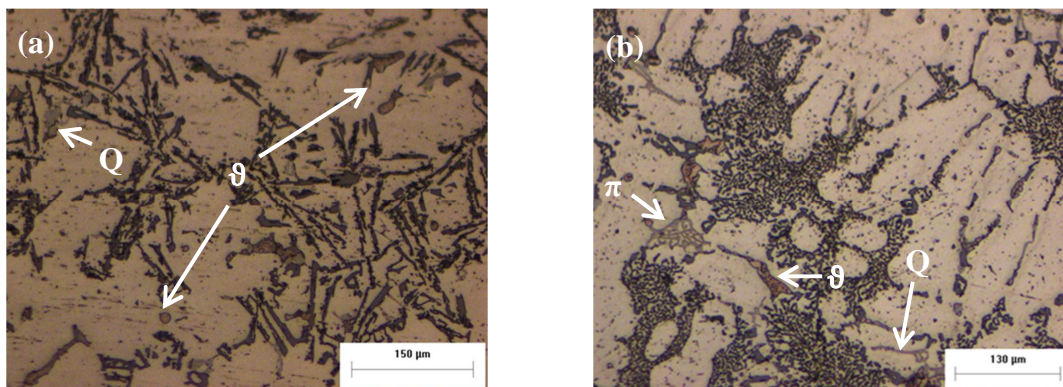


Figure 3.3 - Optical micrographs of A354 alloy without strontium (a) and the same alloy with Sr (b)

The microstructure is characterized by white  $\alpha$ -phase dendrites (that is primary aluminum), which are surrounded by Al-Si eutectic structure (fig. 3.3).

In Fig. 3.3a the eutectic silicon showed an acicular (or needle-like) morphology, which can induce stress intensification in its own apices, reducing the ductility of alloy.

In Fig.3.3b instead the addition of 300 ppm of Sr to the alloy lead to a well modified Si.

The Sr was introduced in melted metal by means of an Al-Sr (10%) master alloy.

Moreover it was possible to distinguish in the interdendritic regions other phases: block-like  $\theta$ -Al<sub>2</sub>Cu phases,  $\pi$  (a light grey compound with an irregular and network-like shape, known as “chinese-script morphology”) and Q (the compact and grey one) particles.

Finally the dark spots observable inside the dendrites are only attributable to the final stage of polish, not to the presence of other particles inside them.

### 3.3.1.2 A354 + 0.1%Mo (casting sequence A)

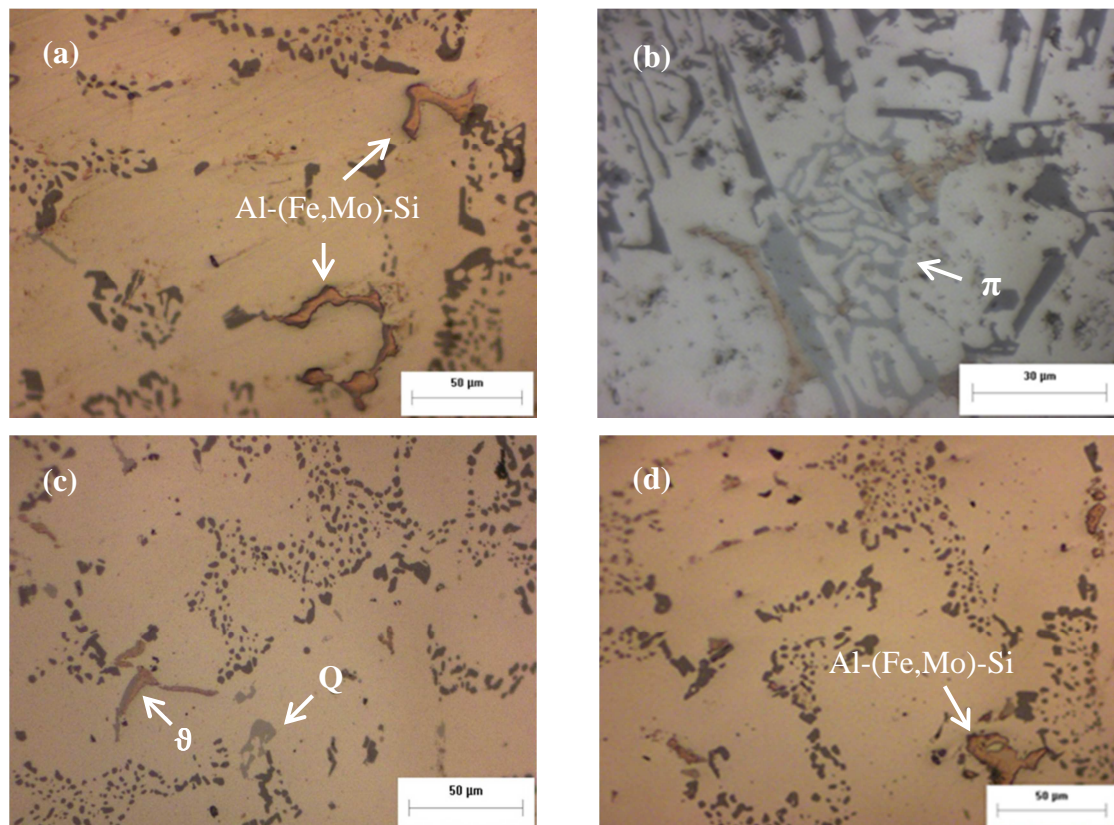


**Figure 3.4 - Optical micrographs of A354 + 0.1% Mo: (a,b) as-cast alloy and (c,d) material microstructure after solution treatment**

No substantial microstructural differences were observed respect to the alloy without Mo except for the presence of molybdenum intermetallics characterised by big dimension and orange colour (fig.3.4c). The analysis confirmed the presence of a well modified

eutectic silicon and of  $\vartheta$  (the round and orange compound), Q (the compact and grey one) and  $\pi$  (the light grey compound with “chinese-script morphology” reported in fig.3.4b). In the specific the image on the top right showed the presence of  $\pi$ -phase, whose formation instead should be suppressed by molybdenum [22], as well as partially unmodified eutectic silicon, which should have been modified by strontium during casting.

No acicular  $\beta$ -phase was instead observed and probably, as suggested by Farkoosh [22], the presence of Mo induces the formation of Al-(Fe,Mo)-Si phase, therefore preventing the nucleation of  $Al_5FeSi$  particles.

As shown in fig.3.4c and d, after complete solution treatment  $\vartheta$  and Q phases were fairly completely dissolved, unmodified eutectic silicon wasn't observed and molybdenum intermetallics didn't show differences and seemed to be unmodified and not solubilized by the treatment (see orange phase in fig.3.4d).

### 3.3.1.3 A354 + 0.3%Mo (casting sequence A)

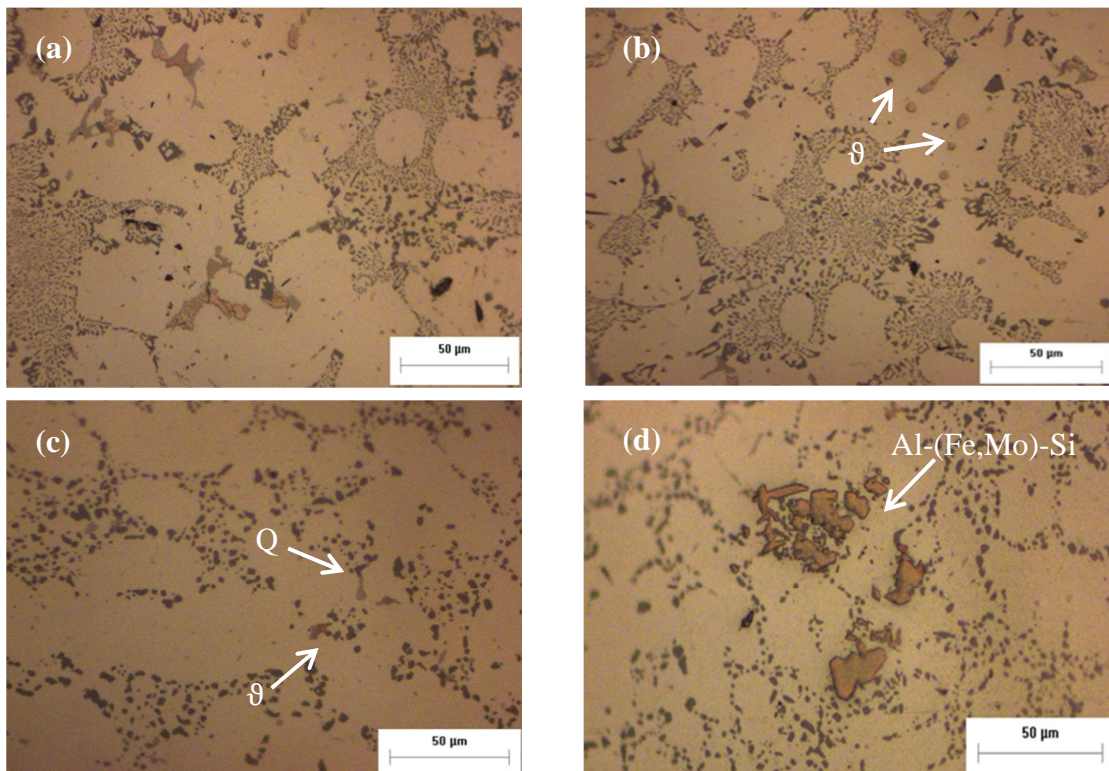


Figure 3.5 - Optical micrographs of A354+0.3% Mo: (a,b) as-cast alloy and (c,d) solution treated alloy

In fig.3.5a and 3.5b  $\theta$  and Q phase could be distinguished, while after solution treatment (as shown in fig.3.5c and 3.5d) they were fairly completely dissolved and appeared really reduced in size.

Conversely fig.3.5d showed the presence of clusters made of molybdenum intermetallics, which weren't affected by heat treatment.

Finally  $\pi$  phase wasn't found, probably as a consequence of higher content in molybdenum, which should hinder its formation [22].

#### 3.3.1.4 A354 + 0.3%Mo (casting sequence B)

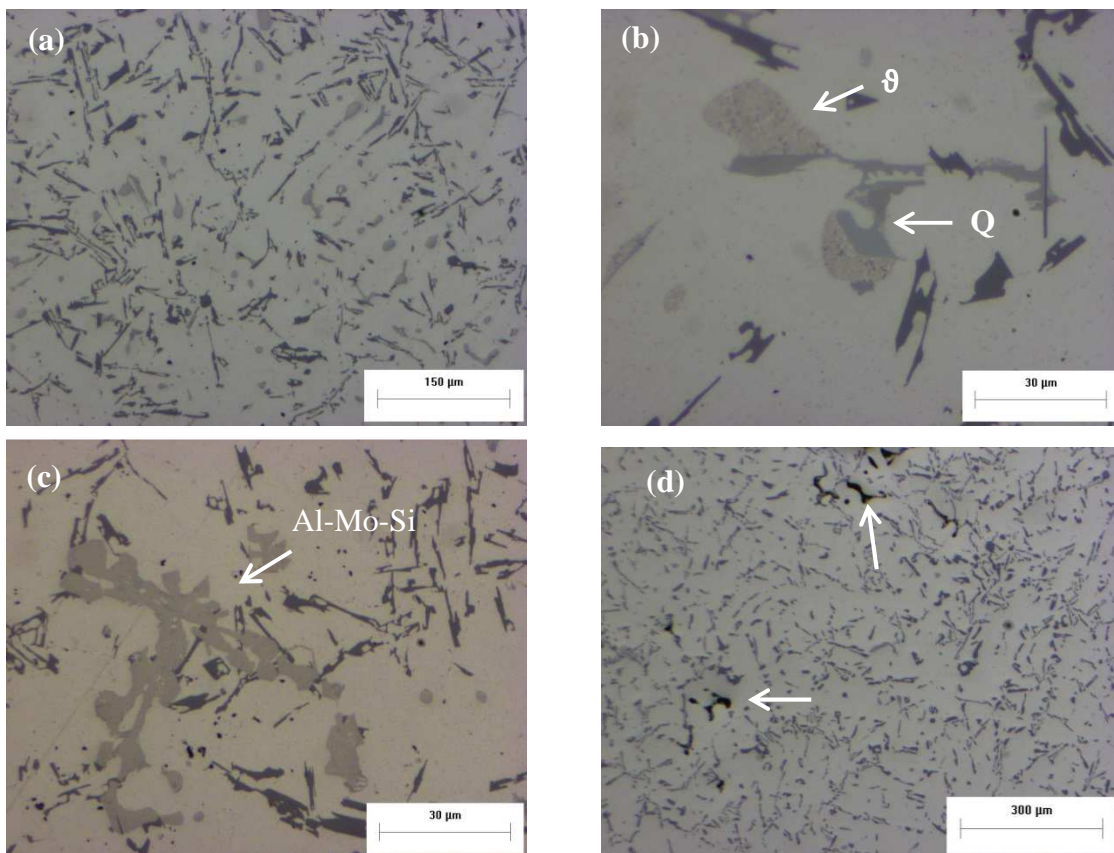


**Figure 3.6 - Optical micrographs of A354 + 0.3% Mo (a, b, c) as-cast and (d) solution treated alloy (small shrinkage cavities highlighted by arrows)**

Firstly, compared to samples casted according casting sequence A, alloy microstructure exhibited differences.

The images 3.6a, b and c presented a not modified eutectic structure regardless the addition of Sr. Only after heat treatment a partial silicon spheroidisation is appreciated (fig.3.6d). Moreover in figure 3.6d showed the presence of small shrinkage cavities.

Fig.3.6c shows how the casting parameters modification has generated differences in Al-Si-Mo phase: instead of being polygonal and orange, it appears light grey-coloured and exhibits a shape similar to a cross.

Probably, due to higher molybdenum diffusion during casting (as a result of 900°C stage), the formation of a different phase was induced.

Furthermore, as for previous samples, figures 3.6a and b recorded the presence of  $\vartheta$  (with a spherical shape) and Q phases.

Solubilized samples showed the substantial disappearance of intermetallics as a natural consequence of heat treatment.

Only a few  $\vartheta$  and Q phases were still detected, but obviously characterised by lower dimensions.

#### 3.3.1.4 A354 + 0.5%Mo (casting sequence A)

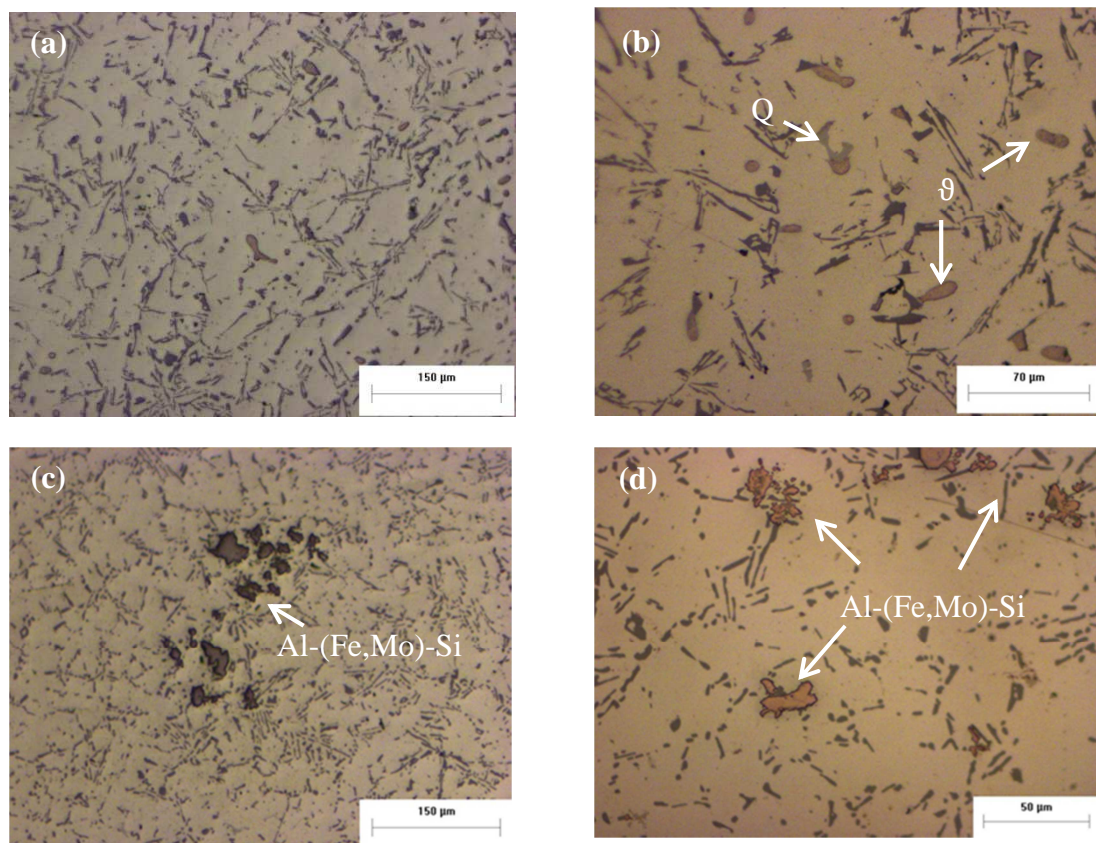


**Figure 3.7 - Optical micrographs of A354 + 0.5% Mo: (a), (b) and (c) represent as-cast alloy, while (c) shows microstructure after solution treatment**

The images 3.7a, 3.7b and 3.7c showed a not modified eutectic structure regardless the addition of Sr. Only after heat treatment a partial silicon modification was appreciated (as shown in fig.3.7d).

Consequently it could be hypothesised that molybdenum in wt.% higher than 0.3 could interfere with strontium, but through mechanisms that were not investigated.

Moreover the as-cast alloy presented  $\vartheta$  and Q phases (fig.3.7a and b), as well as molybdenum clusters (which didn't get modified or partially dissolved) (fig.3.7d).

### 3.3.1.5 A354 + 0.8%Mo (casting sequence A)

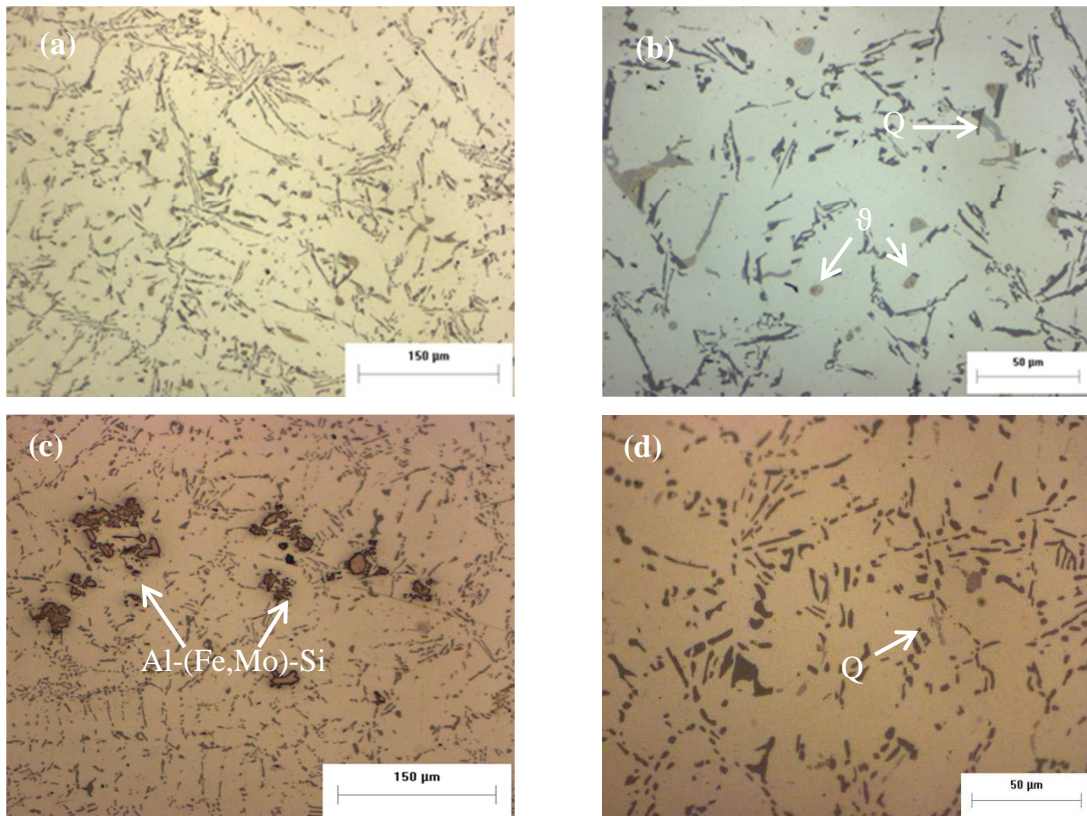
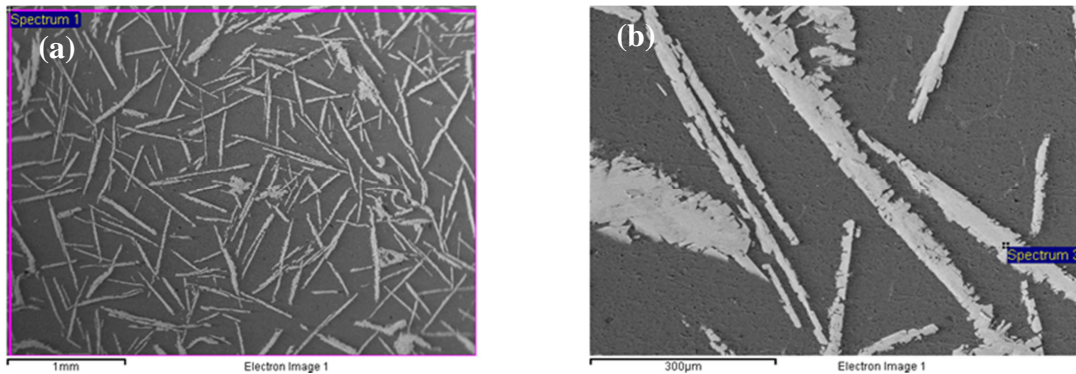


**Figure 3.8 - Optical micrographs of A354 + 0.8% Mo: (a) and (b) represent as-cast alloy, while (c) and (d) show microstructure after solution treatment**

Fig. 3.8a, b and c showed a microstructure similar to that observed for the alloy with 0.5%Mo, confirming that high content in molybdenum interferes with silicon modification and with the formation of  $\pi$  intermetallic. Moreover, as expected, there was an increase of the number and dimension of clusters of molybdenum intermetallics.

### 3.3.2 Scanning electron microscopy

#### 3.3.2.1 Aluminium-molybdenum master alloy



Figures 3.9 – SEM micrographs of aluminium-molybdenum master alloy. In the specific (a) represents a general overview and (b) a detail of Mo-rich phases

Molybdenum master alloy was characterised by needle-like shaped phases rich in Mo of relevant dimensions.

This could explain the difficulties in dissolving it during casting and obtaining a uniform distribution of the alloying element, especially of its intermetallics.

#### 3.3.2.2 A354 + 0.1% Mo (casting sequence A)

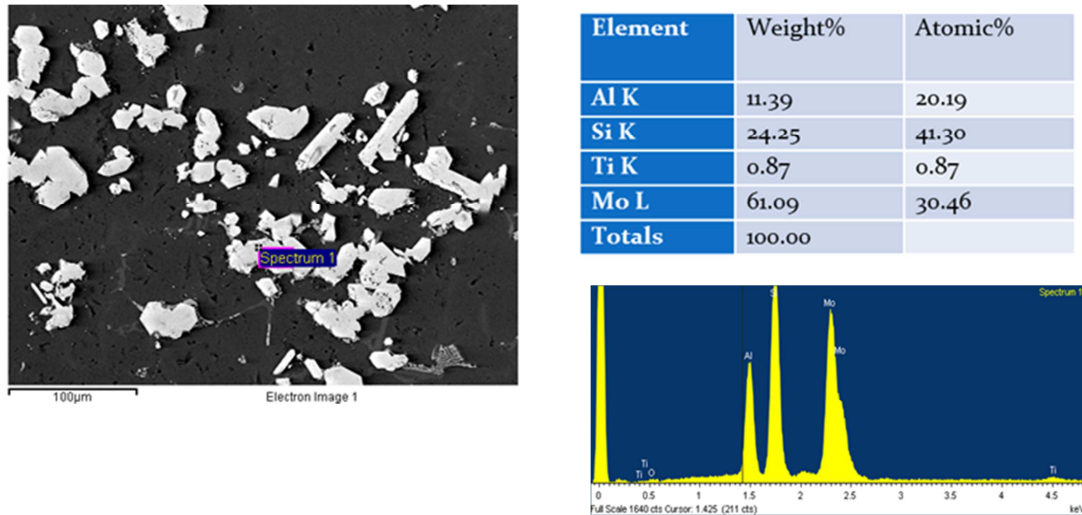
SEM microstructural and EDS analysis highlight only small differences between as cast and heat treated alloy.

In figure 3.10 Mo-based compounds constituted by Al, Si, Mo, Ti can be observed. These could be associated to the phases reported by Farkoosh et al. [22], but characterised by a different composition. In fact they didn't contain iron, but low percentages in titanium, which was detected also in other molybdenum compounds. Moreover the composition and morphology of these intermetallics weren't modified by solution treatment.

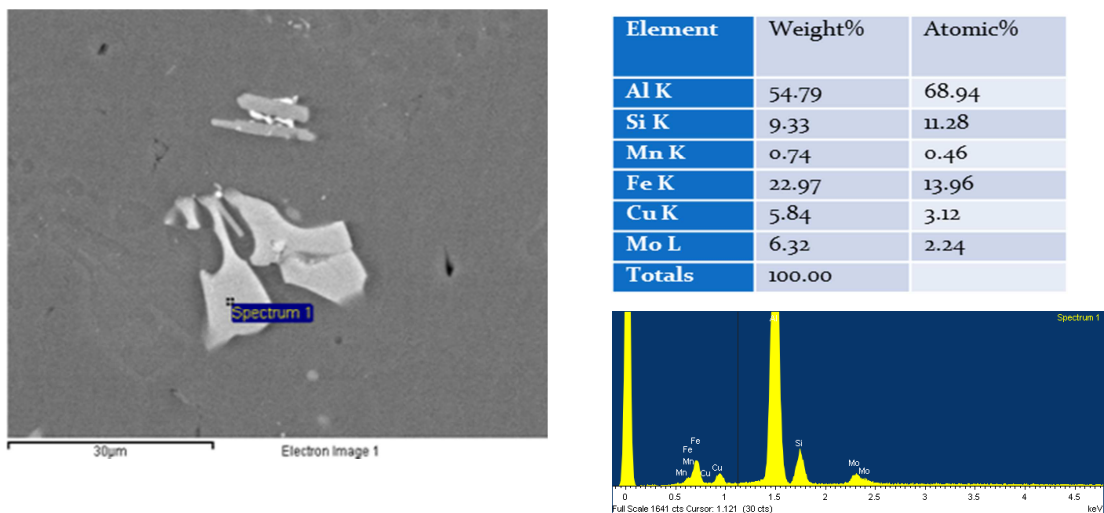
In figure 3.11 instead the Al-(Fe, Mo)-Si phase, also observed by Farkoosh [22], was instead reported.

Q-phase (Al, Si, Cu and Mg) was present both in as cast and heat treated material, but while in as cast sample Q-phase had a well-defined morphology (fig.3.12) in heat treated ones the Q-phase appeared to be fairly completely dissolved (fig.3.13).

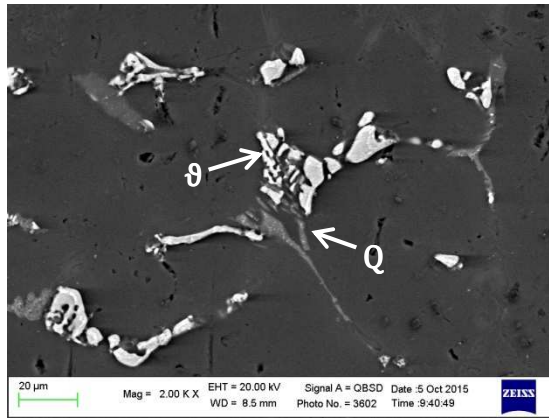
As expected, instead  $\vartheta$ -phase was dissolved during solution treatment and consequently these compounds were present mainly in as cast material, often associated with Q-phase (fig.3.12).



Figures 3.10 – SEM micrographs of a cluster of Mo-rich phases found inside A354+0.1%Mo as cast and corresponding EDS spectrum and chemical composition



Figures 3.11 – SEM micrograph of Al-(Fe,Mo)-Si phase inside heat treated A354+0.1%Mo alloy and corresponding EDS spectrum and chemical composition



Element	Weight%	Atomic%
Al K	45.34	65.74
Si K	0.77	1.07
Cu K	53.89	33.18
Totals	100.00	

Element	Weight%	Atomic%
Mg K	28.10	34.35
Al K	21.98	24.21
Si K	30.65	32.43
Cu K	19.28	9.02
Totals	100.00	

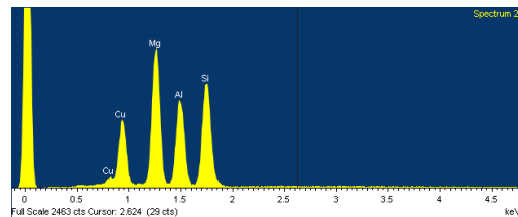
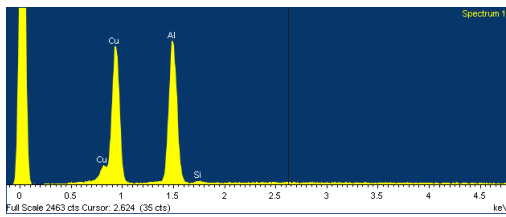
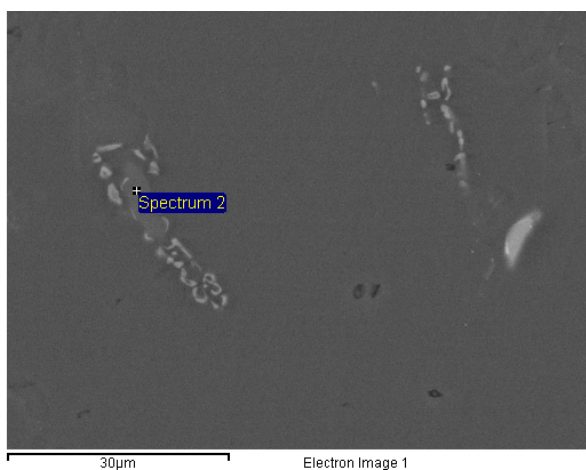


Figure 3.12 – SEM micrographs of  $\theta$  and Q phases in A354+0.1%Mo as cast and corresponding EDS spectra and chemical compositions



Element	Weight%	Atomic%
Mg K	14.20	16.55
Al K	50.34	52.89
Si K	25.18	25.42
Fe K	8.89	4.52
Cu K	1.39	0.62
Totals	100.00	

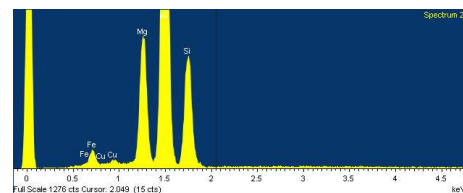


Figure 3.13 – SEM micrographs of Q phase in A354+0.1%Mo after complete solution treatment and corresponding EDS spectrum and chemical compositions

### 3.3.2.3 A354 + 0.3% Mo (casting sequence A)

Through SEM observations it was verified that, even changing molybdenum quantity, alloy microstructure substantially didn't change and moreover no appreciable differences were observed between water quenched and air cooled samples.

In fig. 3.14 molybdenum-rich intermetallics with block-like morphology were reported. Inside them areas with different brightness are observable: thanks to EDS analysis it was verified that higher is molybdenum quantity, lighter they appear.

Moreover it was interesting to verify that also in this compound the content of iron is low and that titanium and vanadium were present, even if they weren't inside molybdenum master alloy.

Therefore it can be supposed that molybdenum interacted with other elements during the formation of these intermetallics through mechanisms that were not investigated.

Unexpectedly alloy microstructure exhibited, even if seldom, two different needle-like phases: little  $\beta$ -Al<sub>5</sub>FeSi particles (fig.3.15), whose formation should be theoretically suppressed by molybdenum and Mo-based ones, which are identified as acicular molybdenum-rich phases from master alloy (fig.3.16) not completely dissolved during casting.

The presence of the latter made rethink casting stage and modify its process parameters, adding 900°C stage in order to homogenize molybdenum inside alloy.

Finally figure 3.17 showed the presence of  $\theta$ -CuAl<sub>2</sub> (the lighter phase) and Q (the darker one) intermetallics, whose formations are often associated.

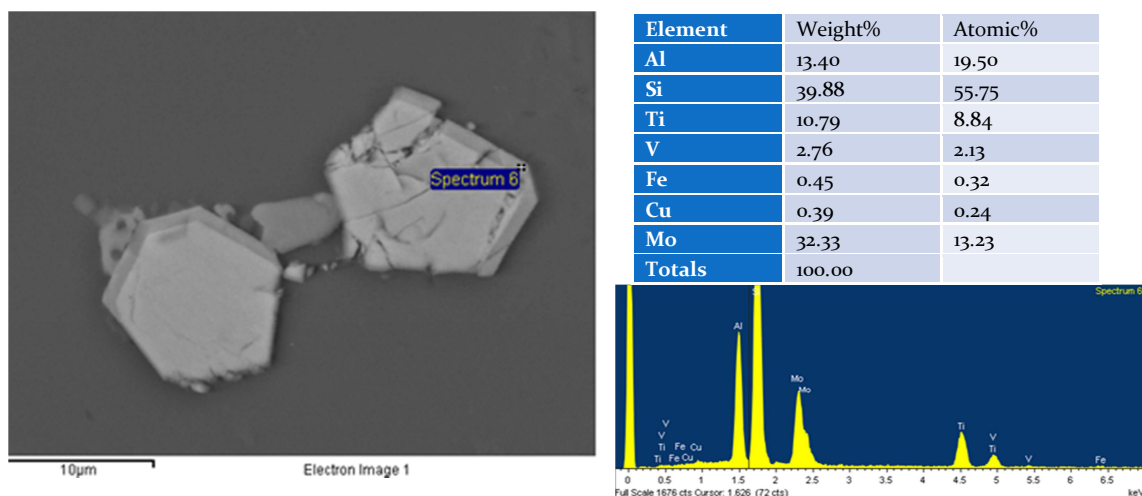
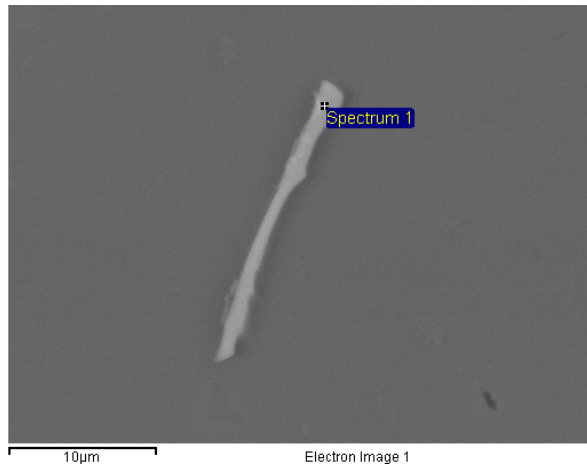


Figure 3.14 - SEM micrograph of a Mo-rich phase inside A354+0.3%Mo as cast and corresponding EDS spectrum and chemical composition



Element	Weight%	Atomic%
Al K	67.14	78.50
Si K	7.63	8.57
Mn K	0.39	0.22
Fe K	15.92	8.99
Cu K	4.65	2.31
Mo L	4.27	1.41
Totals	100.00	

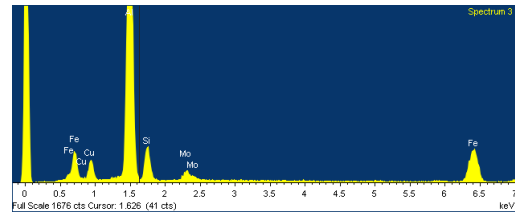
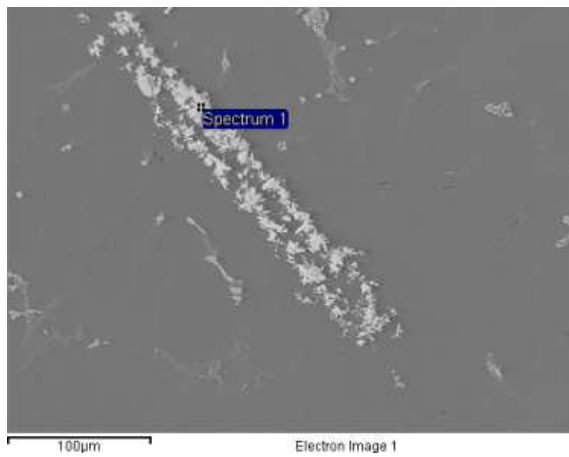


Figure 3.15 - SEM micrograph of  $\beta$ -Al<sub>5</sub>FeSi phase inside A354+0.3%Mo as cast and corresponding EDS spectrum and chemical composition



Element	Weight%	Atomic%
Al K	11.38	20.41
Si K	26.76	46.11
Ti K	2.92	2.95
V K	0.40	0.38
Fe K	0.42	0.36
Cu K	1.79	1.37
Mo L	56.32	28.41
Totals	100.00	

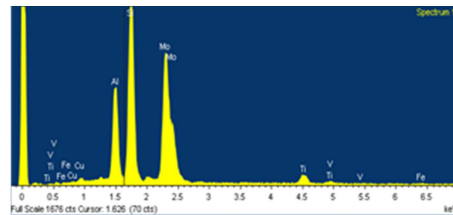
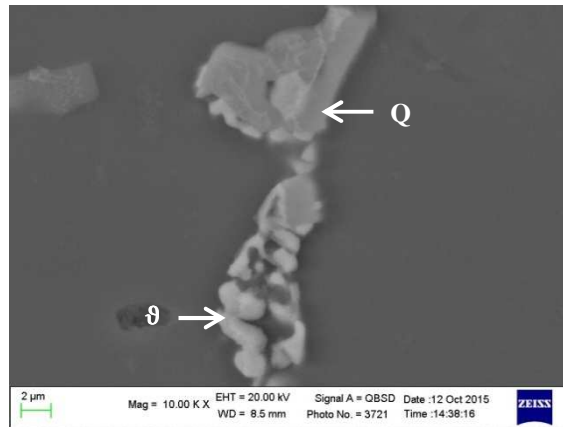


Figure 3.16 – SEM micrographs of Mo-rich phase found inside A354+0.3%Mo as cast and corresponding EDS spectrum and chemical composition



Element	Weight%	Atomic%
Mg K	1.90	2.63
Al K	55.36	69.28
Si K	8.00	9.62
Cu K	34.75	18.47
Totals	100.00	

Element	Weight%	Atomic%
Al K	54.47	68.69
Si K	9.29	11.26
Fe K	22.60	13.77
Cu K	7.98	4.27
Totals	100.00	

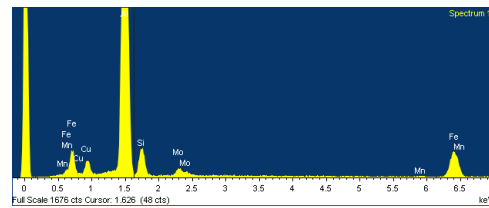
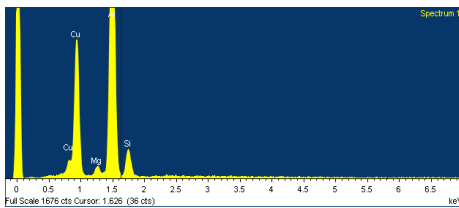


Figure 3.17 - SEM micrograph of  $\theta$  and Q phases found inside A354+0.3%Mo as cast and corresponding EDS spectra and chemical compositions

### 3.3.2.4 A354 + 0.3% Mo (casting sequence B)

As shown previously by optical micrographs (fig 3.6), casting sequence B (which guarantees higher molybdenum diffusion) didn't modify morphology of Mg and Cu-based particles, while induces changes in Mo phases.

The microstructure of solutioned alloy was characterized by the presence of Mo-based intermetallics, since Cu and Mg-based phases were fairly completely dissolved during heat treatment.

Two different morphologies of Mo-containing compounds were found, which substantially differed according to iron content: block-like particles, constituted of Al, Si, Fe and Mo, were mostly observed in interdendritic regions, also in association with other

intermetallics (in particular  $\vartheta$  phase), as shown in fig. 3.19; while cross-like ones, containing only Al, Mo and Si, were usually located within the  $\alpha$ -Al region (fig. 3.20).

In figure 3.19 it was possible to distinguish a series of compounds, whose formation seemed to be associated: compact molybdenum compound (which is different from that reported below with cross-shaped morphology),  $\vartheta$  phase and  $\pi$  intermetallic (which had polygonal morphology, instead of classic chinese-script one).

Compared to alloy casted according casting sequence A, no  $\beta$  particles were observed.

Probably the higher molybdenum diffusion let interact and react with iron, preventing from the nucleation of  $\beta$ -Al<sub>5</sub>FeSi particles.

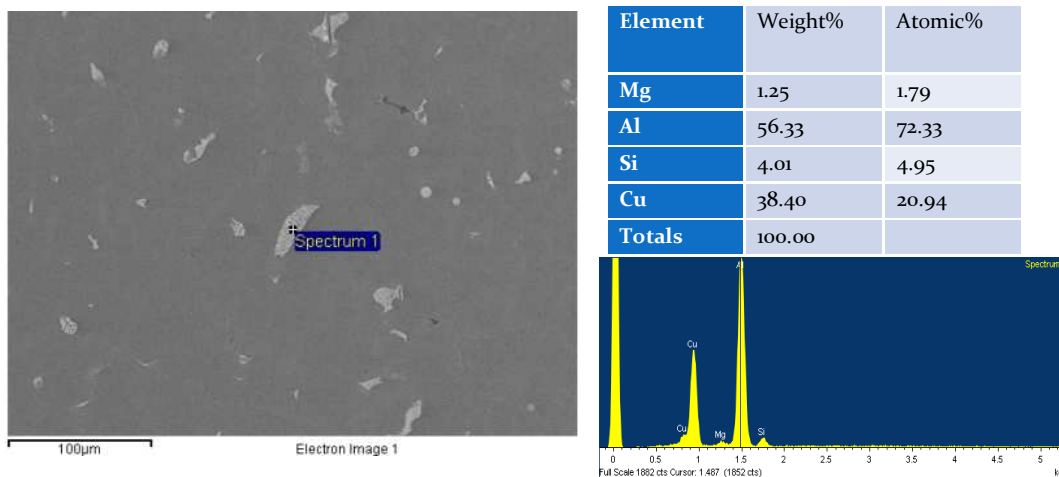


Figure 3.18 - SEM micrograph of  $\vartheta$  phase inside A354+0.3%Mo as cast and corresponding EDS spectrum and chemical composition

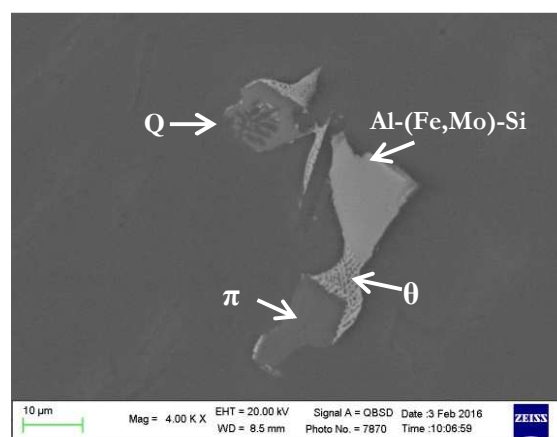
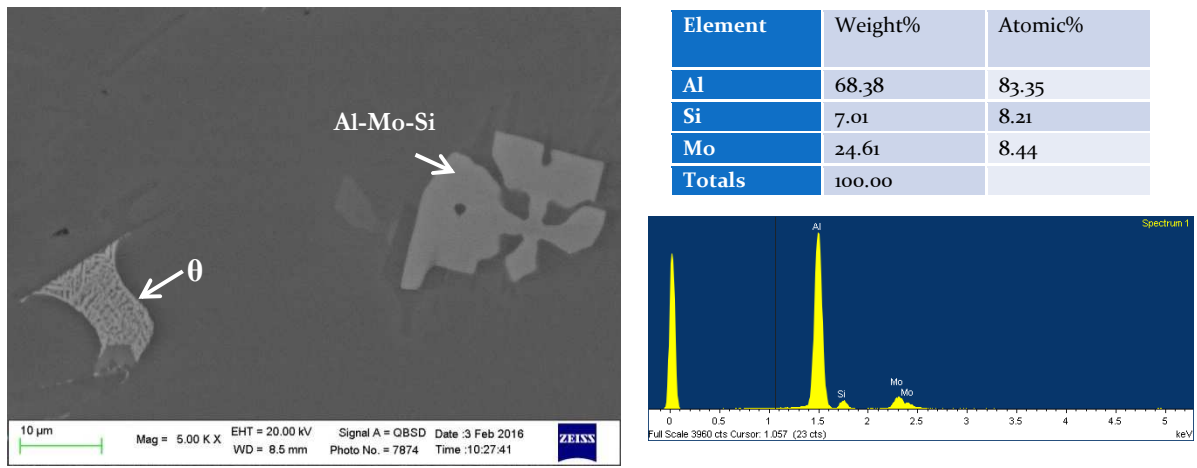


Figure 3.19 - SEM micrograph of  $\vartheta$ , Q,  $\pi$  and Al-(Fe,Mo)-Si phases inside A354+0.3%Mo as cast and corresponding EDS spectra and chemical compositions



**Figure 3.20 - SEM micrograph of phases found inside A354+0.3%Mo as cast and corresponding EDS spectrum and chemical compositions**

### 3.4 Secondary Dendrite Arm Spacing (SDAS) measurement

The average SDAS values are reported in table 2.5.

Mo %wt	Mould temperature (°C)	SDAS (μm)
0.1	300	39 ± 13
0.3	200	26 ± 5
0.5	200	31 ± 3
0.8	200	32 ± 6

**Table 2.5 - Average SDAS values of A354 alloy with different percentages in molybdenum**

The alloys containing Mo wt% between 0.3 and 0.8 showed similar SDAS values ranging between 26 and 32 μm, while the alloy with 0.1wt% of Mo has higher SDAS. This difference is however a consequence of the higher die temperature and not of the low Mo amount. Mo, in fact, doesn't seem have influence on SDAS [24, 25].

### 3.5 Hardness measurements

Hardness measures were carried out on specimens casted according to casting sequence A.

### 3.5.1 Macrohardness measurements

The values obtained as a result of several series of measures are reported as follows in diagrams below.

Macrohardness values are recorded in tables “A.2, A.3, A.4, A.5, A.6” of “Appendix” section.

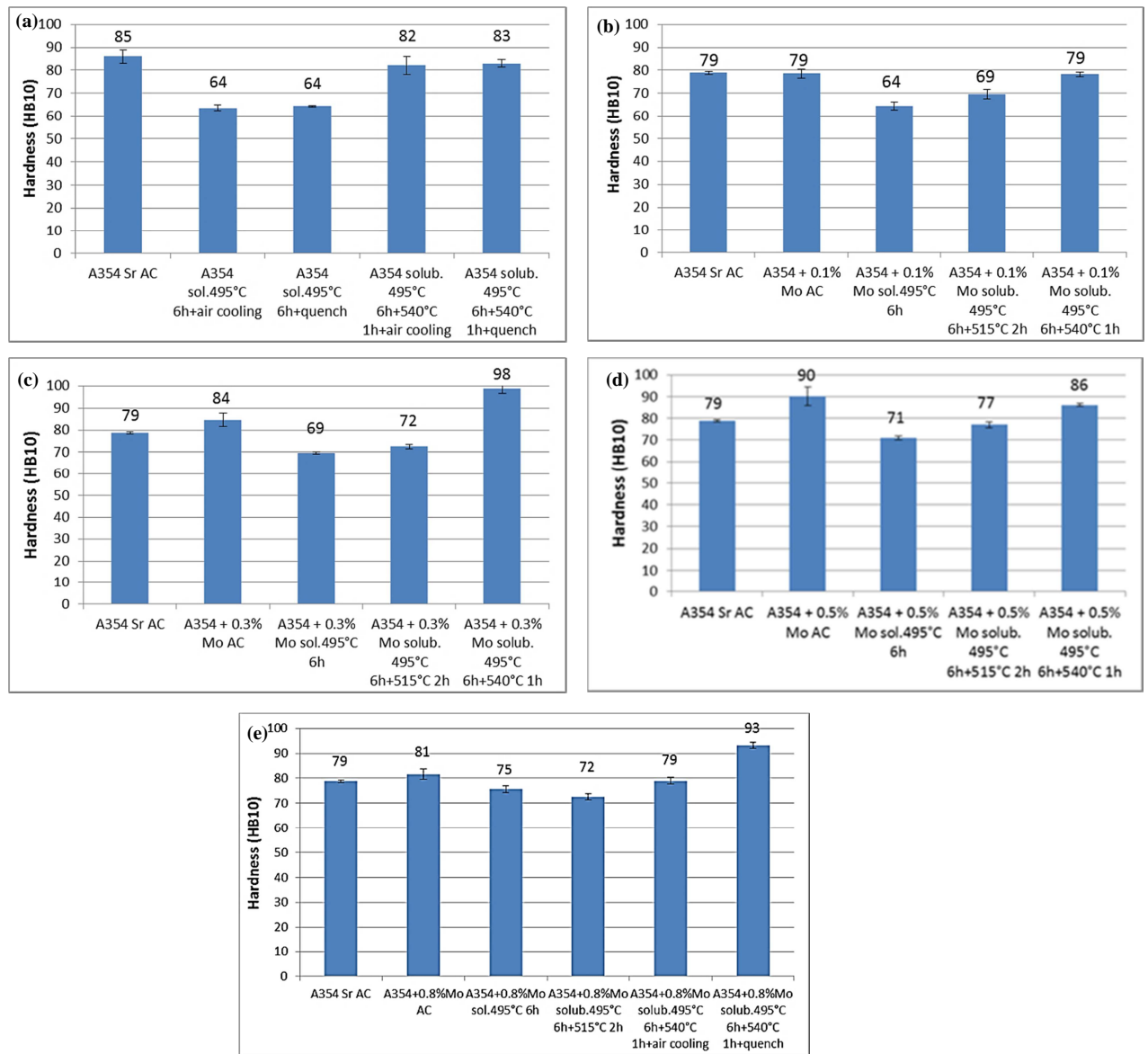


Figure 3.21 – Macrohardness values of A354 base alloy and A354 modified with (a) 0.1, (b) 0.3, (c) 0.5 and (d) 0.8% in Mo at different heat treatment stages (from as cast to complete solution treatment). In particular, where not specified, the samples were quenched after solubilisation

Despite of different content in molybdenum, the hardness showed a similar trend: as cast alloys presented values of about 80 HB<sub>10</sub>, then, as a consequence of first phase of

solution treatment at 495°C, these decreased and finally an increase after solubilisation at higher temperature was recorded.

In particular, if solution treatment was conducted at 540°C, better performances were registered in molybdenum-containing alloys.

This indicated, as reported by [22], that compared to 515°C, soaking at 540°C induced higher mobility to the Mo solutes, enabling the precipitation of the dispersoids.

The only difference were observed in A354 base alloy and A354+0.1%Mo, in which after heat treatment phase at 540°C hardness values didn't have a relevant increase.

This confirm that the enhancement of hardness values of the alloy with Mo after complete solution treatment could be due to the development of dispersoids, which in the A354 alloy isn't present, while in the A354+0.1%Mo the Mo percentage is too low for appreciating its effect.

### 3.5.2 Microhardness measurements

The values obtained as a result of several series of measures are reported as follows in diagrams below.

Microhardness values are recorded in tables “A.7, A.8, A.9, A.10” of “Appendix” section.

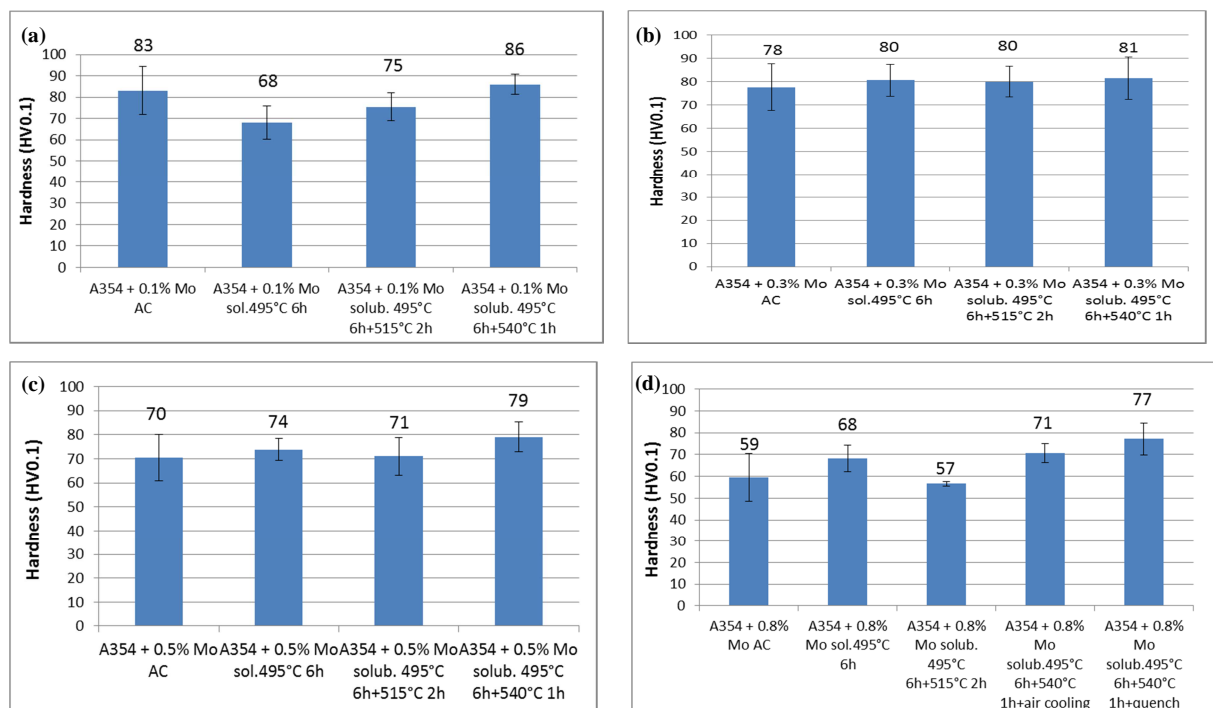


**Figure 3.22 - Microhardness values of A354 alloy modified with (a) 0.1, (b) 0.3, (c) 0.5 and (d) 0.8% in Mo at different heat treatment stages (from as cast to complete solution treatment). In particular, where not specified, the samples were quenched after solubilisation**

The microhardness trends were similar to those observed for macrohardness.

However it is important to notice that, while microhardness measures were carried out locally in the  $\alpha$ -phase and could be influenced by harder compounds (present around or under the  $\alpha$  one), Brinell ones determined an average value of all the microstructural constituents of the alloy.

Consequently, despite of several measures performed on the samples, standard deviation values of microhardness were higher than those of macrohardness tests.

### 3.6 Ageing curves

In figure 3.23 ageing curves obtained at 180°C for the alloys solution treated both at 515 and 540°C are reported.

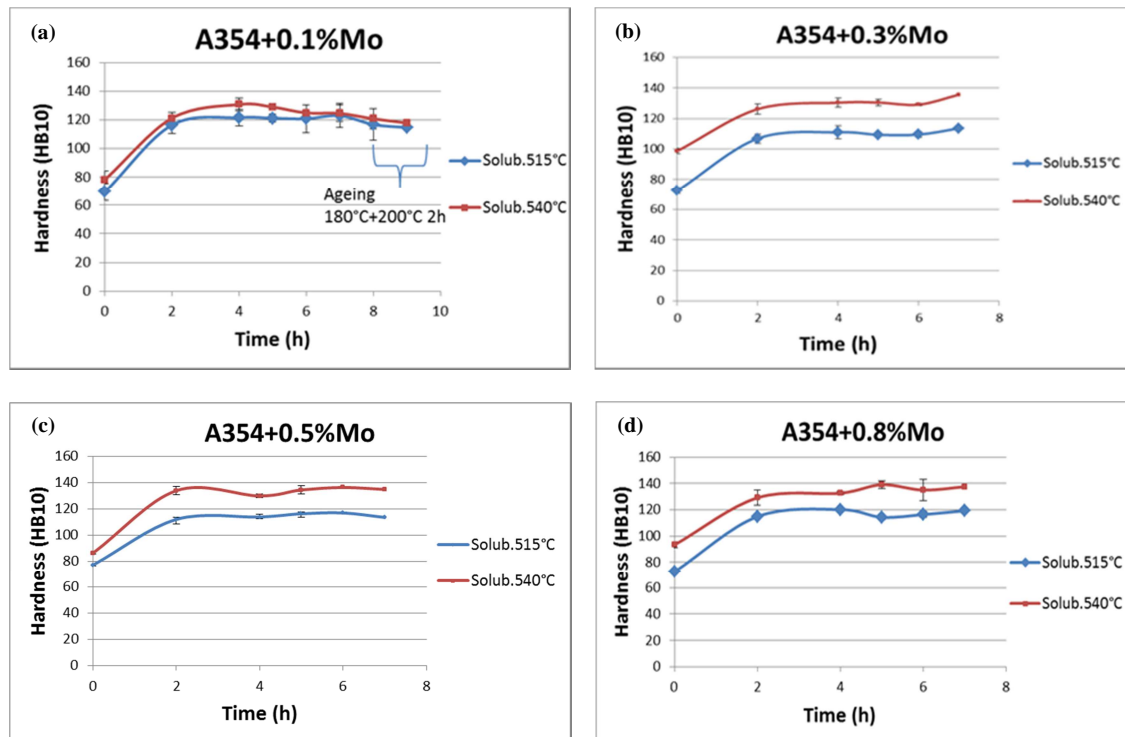


Figure 3.23- Ageing curves of A354 alloy with different molybdenum content after solution treatments at 515°C for 2h and 540°C for 1h. In the specific (a) 0.1%, (b) 0.3%, (c) 0.5%, (d) 0.8% in Mo

The diagrams highlighted the greater effectiveness of 540°C solution treatment, which allowed to reach in the alloys, after aging, higher hardness (about 10-20 HB) compared to alloys subjected to solution at 515°C.

Only A354 with 0.1% in Mo showed a smaller gap between the two curves, probably due to the lower content in molybdenum and consequently lower influence on the heat treatment results.

Moreover it could be noticed that the highest results for molybdenum-containing alloys were obtained already after 4 h, instead of 7, as reported for A354 without Mo [24, 25].

### **3.7 High temperature exposure**

The diagrams were obtained as a result of a series of measures made at specific time intervals, analysing samples containing the same percentage of molybdenum and subjected to different treatment after solubilisation (air cooling, quench, quench + ageing) and comparing the results.

#### **3.7.1 Solution treatment 495°C for 6h + 540°C for 1h+soaking 245°C for 301h:**

A354 samples underwent T6 heat treatment with the following parameters: solution treatment for 6h at 495°C + for 2h at 515°C + quench (water at 60°C) + ageing for 7h at 180°C (the heat treatment developed from [24, 25]). This data was used only as a comparison term, whose results were already known and available.

No substantial differences were recorded between A354 alloy with or without molybdenum, with the residual hardness stabilised at 65-70 HB10. Only the alloy containing 0.1% in Mo showed a residual hardness lower than 60HB10.

The heat treatment (air cooling, quench or quench + ageing) influenced the hardness curves only in the first phase of the high temperature exposition, while it doesn't appreciably affects the residual hardness after 300h.

In particular ageing effects seemed to fade after some days at high temperature. Moreover it appeared that higher content in molybdenum induced a smaller gap between aged and non-aged samples.

High temperature exposure acted as over-ageing for T6 treated samples and, probably, as rapid aging (that can't be appreciated, because first hardness measurements were carried out after 301h) + over-ageing for solubilised and quenched or air cooled ones. This led to the evolution of the strengthening precipitates from coherent to incoherent morphology, their coarsening and consequent reduction in hardness value.

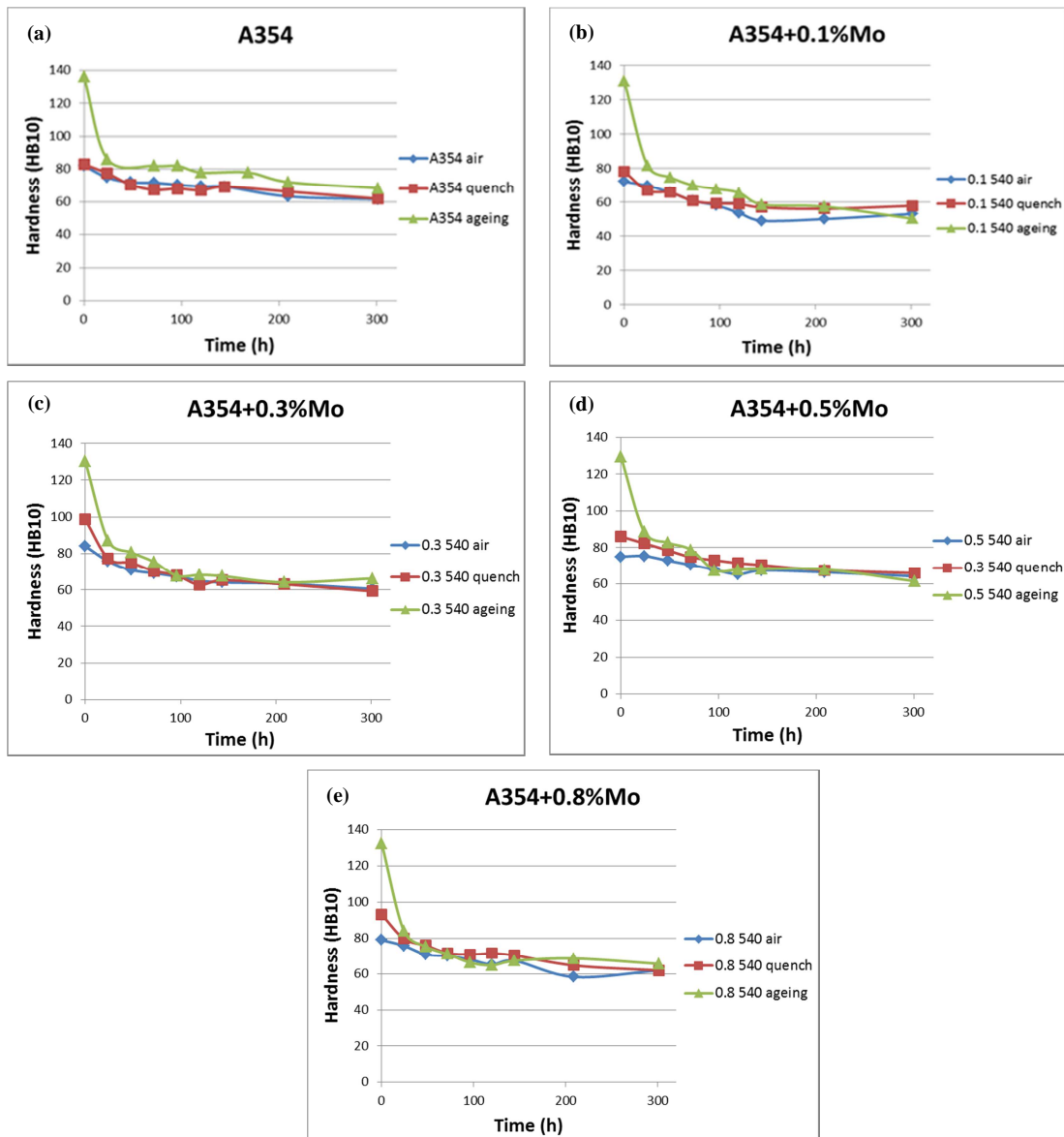
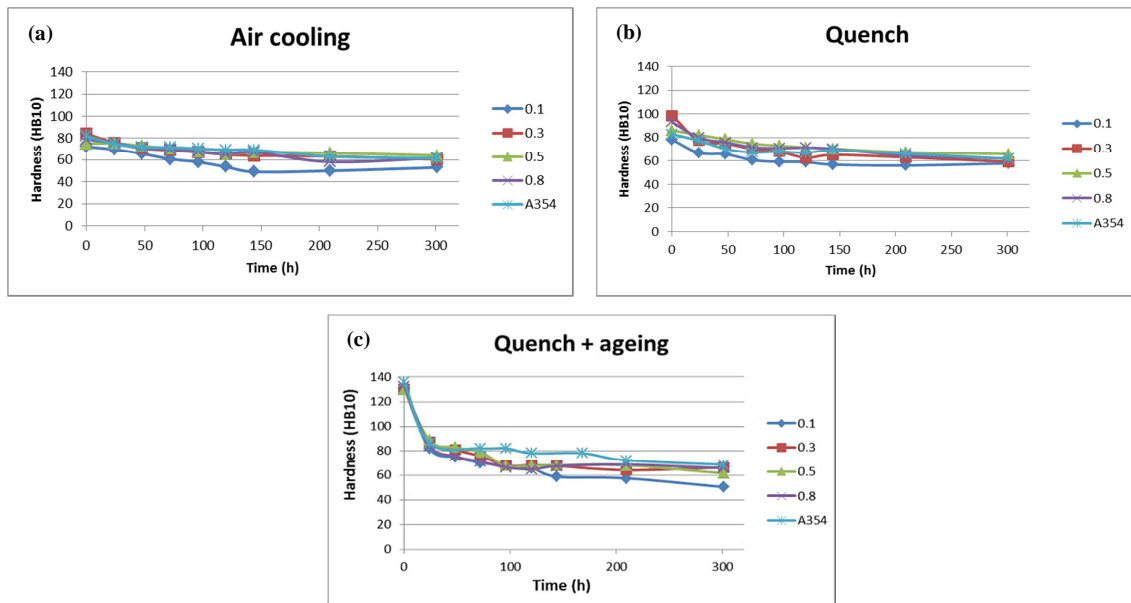


Figure 3.24 – Over-ageing curves (245°C for 301h) of A354 alloy with different molybdenum contents subjected to air cooling, quench and quench + ageing after complete solution treatment. In the specific (a) A354 without Mo, (b) 0.1%, (c) 0.3%, (d) 0.5% and (e) 0.8% in Mo

Arranging instead the data according to the treatment undergone after solubilisation, the resulting diagrams showed the following outcome:



**Figure 3.25 – Over-ageing curves (245°C for 301h) of A354 alloy with different molybdenum contents subjected to (a) air cooling, (b) quench and (c) quench + ageing after complete solution treatment. Every image compares the results of A354 alloy with different percentages in Mo undergone to different treatment after solubilisation**

The diagrams showed that, despite the same alloys were subjected to three different treatment after solubilisation (air cooling, quench and quench + ageing), they reached the same residual hardness after high temperature exposition.

These results made suppose that heat treatment limited to air cooling could be sufficient to have good performances over time and this would mean a notable advantage both economically (the heat treatment would be composed by less phases) both in terms of fatigue behaviour (the quench phase is often critical and generates residual stresses, which are negative for the application of materials).

### **3.7.2 Solution treatment 495°C for 6h + 540°C for 1h + soaking 245°C for 120h + 300°C for 42h:**

Copper and magnesium intermetallics (remained in small part after solution treatment) and precipitates can only be effective for strength and creep resistance below 250°C, because above this temperature they start to become unstable, coarsen rapidly (due to Ostwald ripening) and then dissolve [12].

As previously viewed, despite of higher degradation temperature, A354 seemed to reach similar performances, both with both without molybdenum.

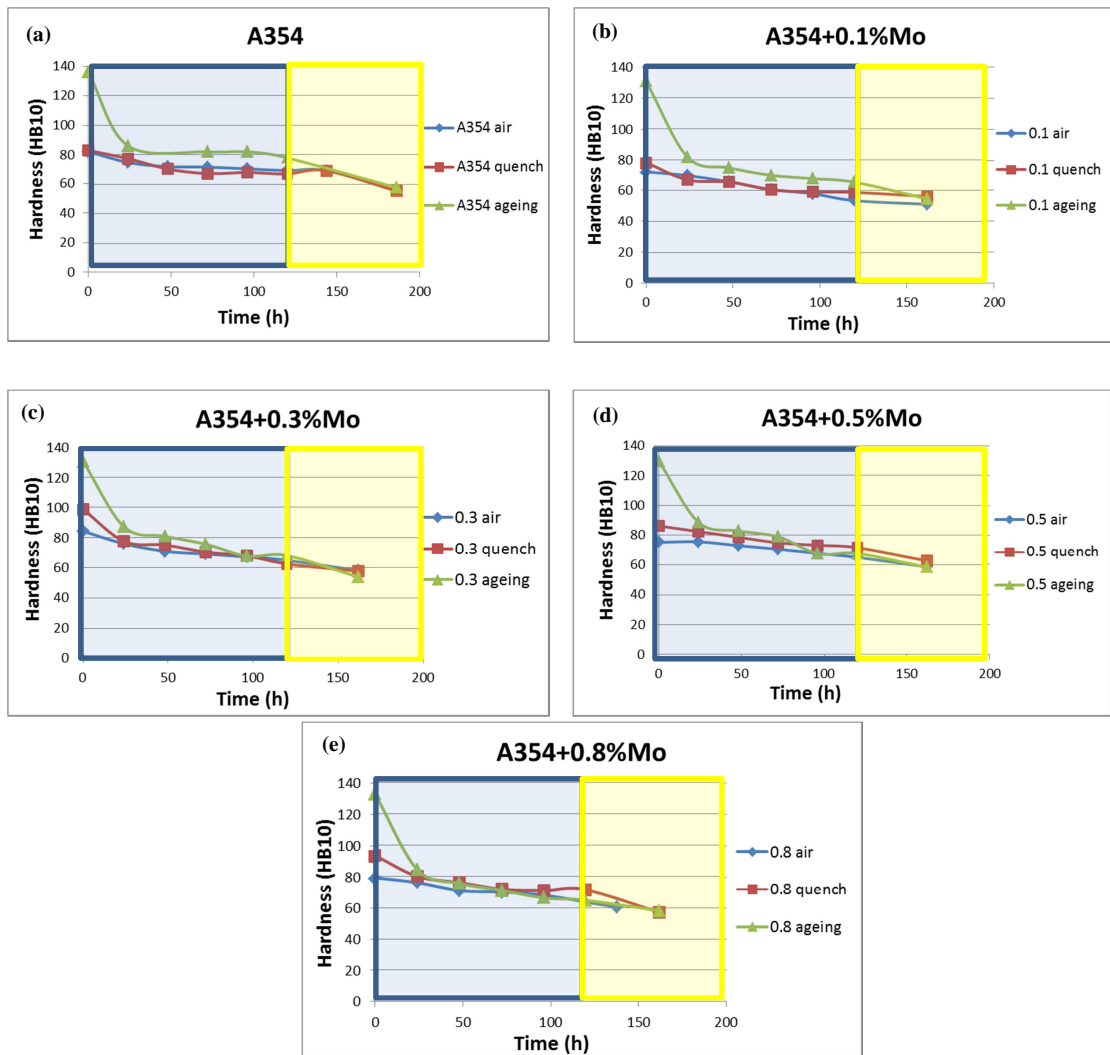


Figure 3.26 – Over-ageing curves (245°C for 120h + 300°C for 42h) of A354 alloy with different molybdenum contents subjected to air cooling, quench and quench + ageing after complete solution treatment (495°C for 6h + 540°C for 1h). In the specific (a) A354 without Mo, (b) 0.1%, (c) 0.3%, (d) 0.5% and (e) 0.8% in Mo. Blue region corresponds to over-ageing at 245°C, while yellow one to treatment at 300°C

In fig. 3.27 the results are summarised according to the treatment undergone after solubilisation.

As previously viewed for degradation at 245°C, the data demonstrated that alloys reached the same performances over a long period of time, making suppose that air cooling after solution treatment would be sufficient for application in temperature.

In fact the only persistent reinforcement phases would be the molybdenum ones (that is intermetallics and dispersoids) [22].

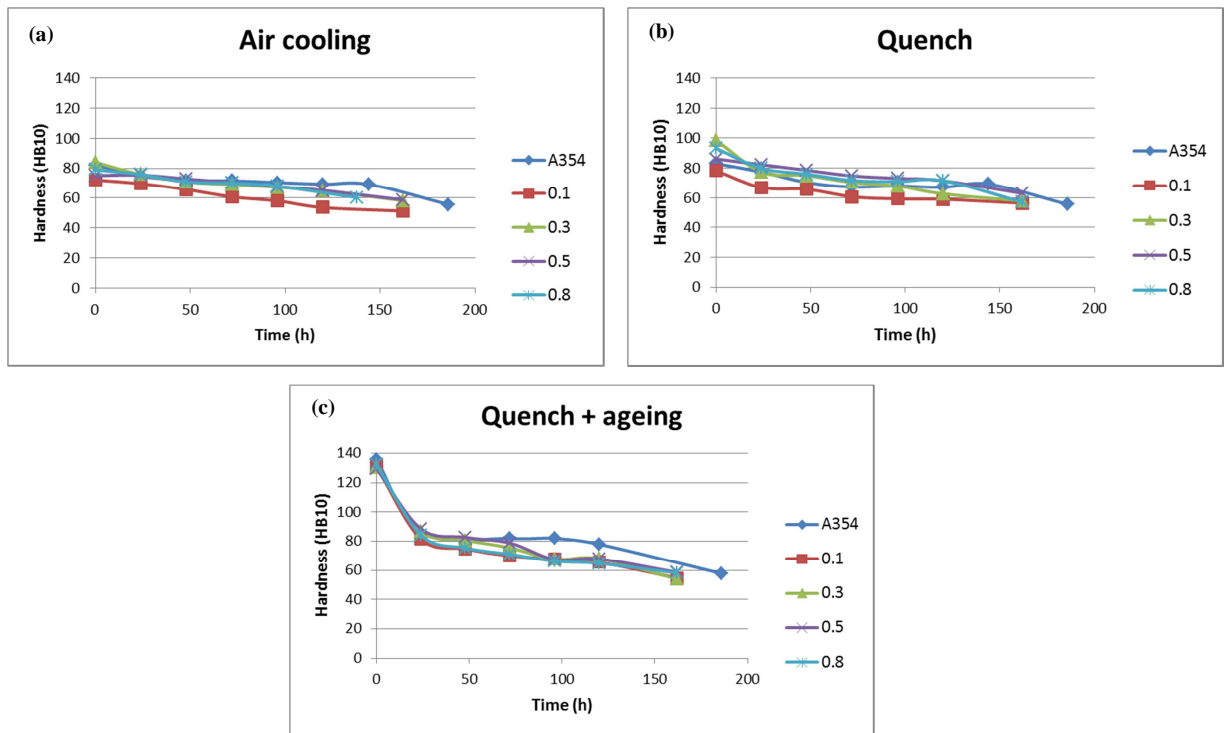


Figure 3.27 – Over-ageing curves (245°C for 120h + 300°C for 42h) of A354 alloy with different molybdenum contents subjected to (a) air cooling, (b) quench and (c) quench + ageing after complete solution treatment (495°C for 6h + 540°C for 1h). Every image compares the results of A354 alloy with different percentages in Mo undergone to different treatment after solubilisation

### 3.7.3 Solution treatment 495°C for 6h + 540°C for 10h + soaking 245°C for 144h:

Finally, in order to compare performances induced by different time of solution treatment, A354 and A354+0.3%Mo alloys underwent degradation after solubilisation of 6 hours at 495°C and 10 hours at 540°C. The results are reported in Fig.3.28.

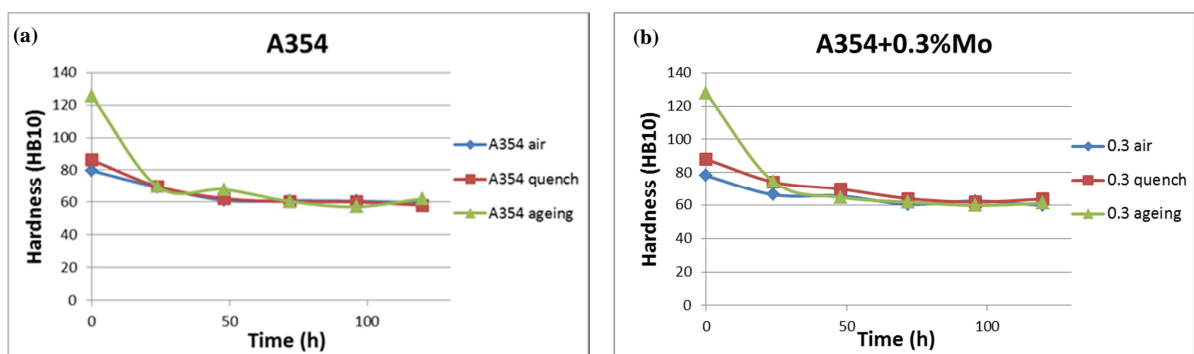
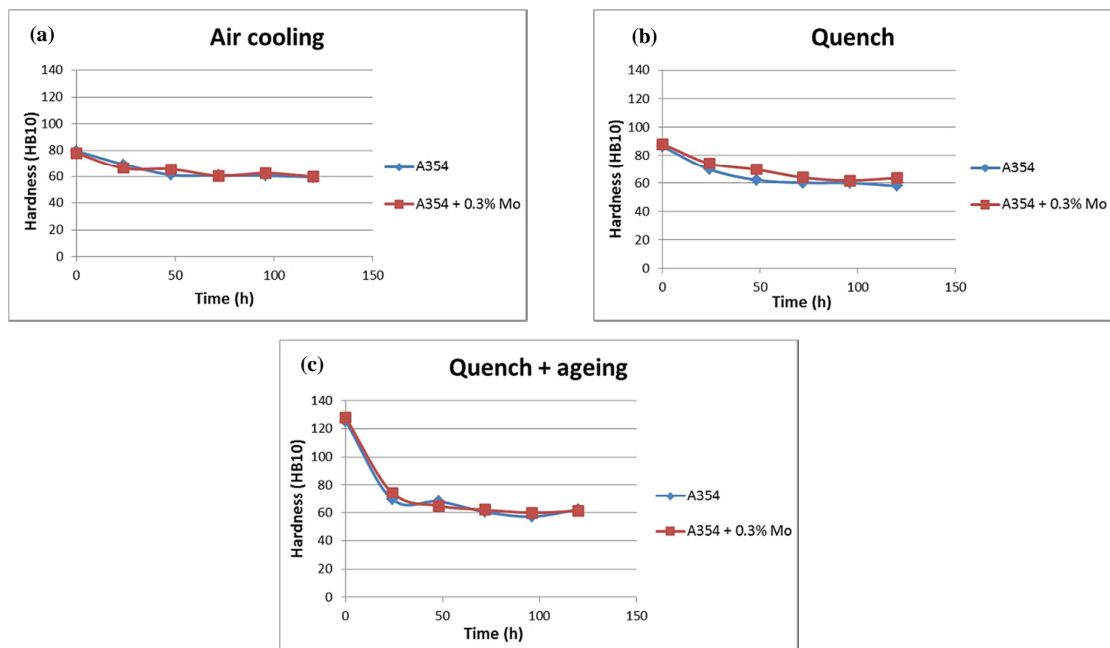


Figure 3.28 – Over-ageing curves (245°C for 144h) of A354 alloy with different molybdenum contents subjected to air cooling, quench and quench + ageing after complete solution treatment (495°C for 6h + 540°C for 10h). In the specific (a) A354 without Mo and (b) 0.3% in Mo

After different heat treatment the samples reached performances lower than the previous ones with a gap of about 5-10 HB10.

Then it could be asserted that longer solution treatment had a negative influence on material and this might be attributed to the coarsening of the molybdenum dispersoids, which would have reduced high temperature resistance of the alloy.

In fig. 3.29 data are reported according to the treatment undergone after solubilisation.



**Figure 3.29 – Over-ageing curves (245°C for 144h) of A354 alloy without Mo and with 0.3% in Mo subjected to (a) air cooling, (b) quench and (c) quench + ageing after complete solution treatment. Every image compares the results of A354 and A354 + 0.3%Mo undergone to different treatment after solubilisation**

As shown by previous graphs no great differences were recorded between alloys air cooled, quenched or aged, making suppose an employment of the material without the usual complete heat treatment with relevant cost savings.

### 3.8 Tension tests

As a consequence of metallographic analysis, DSC, hardness and degradation data, as well as information from literature, it was established to concentrate the study on A354 modified with 0.3% in molybdenum, in order to compare it with base alloy.

Therefore tension tests were carried out on samples of A354 base alloy and A354+0.3%Mo, which were tested in different condition (see table 2.4) after complete solution treatment.

The results are presented in table 3.30.

Samples designation	Treatment undergone	Test conditions	Yield strength (MPa)	Ultimate strength (MPa)	Elongation measured (E%)
A T6	Solution treatment (495°C 6h + 540°C 1h) + quench + ageing (180°C 6h)	Room temperature	285 ± 14	380 ± 19	2.6 ± 0.1
A OA	Solution treatment (495°C 6h + 540°C 1h) + quench + ageing (180°C 6h) + over-ageing at 250°C for 100h	250°C	93 ± 5	117 ± 6	12.3 ± 6.1
MoA	Solution treatment (495°C 6h + 540°C 1h) + air cooling + ageing (180°C 6h)	Room temperature	187 ± 9	281 ± 14	6.4 ± 0.3
MoA OA	Solution treatment (495°C 6h + 540°C 1h) + air cooling + ageing (180°C 6h) + over-ageing at 250°C for 100h	250°C	89 ± 4	129 ± 6	19.4 ± 1.0
MoT	Solution treatment (495°C 6h + 540°C 1h) + quench + ageing (180°C 6h)	Room temperature	322 ± 16	367 ± 18	3.5 ± 0.2
MoT OA	Solution treatment (495°C 6h + 540°C 1h) + quench + ageing (180°C 6h) + over-ageing at 250°C for 100h	250°C	103 ± 5	130 ± 6	16.7 ± 0.8

**Table 3.30 - Tensile properties of A354 alloy (A), A354+0.3%Mo alloy solubilised, air cooled and aged (MoA), A354+0.3%Mo alloy solubilised, quenched and aged (MoT)**

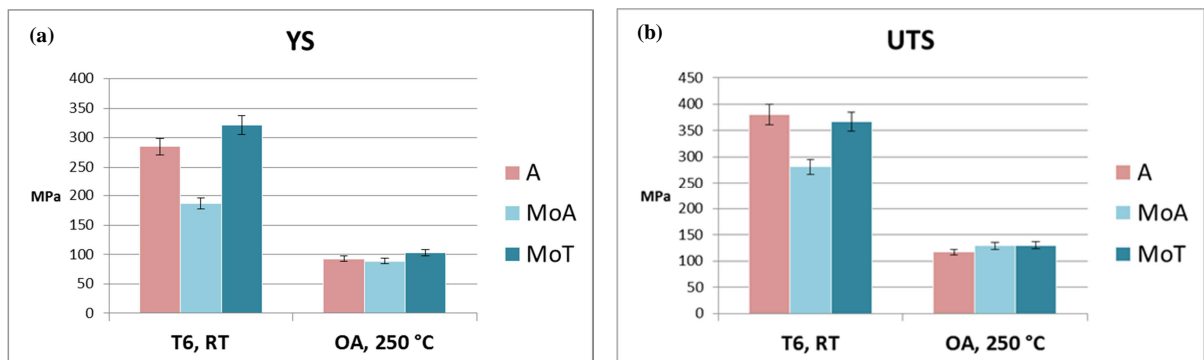


**Figure 3.30 – Tensile properties (YS=yield strength; UTS=ultimate tensile strength) of A354 alloy (A), A354+0.3%Mo alloy solubilised, air cooled and aged (MoA), A354+0.3%Mo alloy solubilised, quenched and aged (MoT). In particular “RT” means that tests were carried out at room temperature, while “OA” identifies samples exposed at high temperature (100h at 250°C) and tested at 250°C**

As shown by fig.3.30 the presence of molybdenum at room temperature induced an increase of the YS of about the 10% while its influence on UTS was negligible; at 250°C,

instead, both YS and UTS of samples with Mo were higher (about 10%) respect to samples without Mo.

The enhancement in mechanical properties was attributed to the presence of Mo dispersoids, which hinder dislocation movements. This effect was particularly interesting for high temperature tests, in which the contribution of  $\theta$  and Q phases was weak, due to their coarsening and dissolution.

Moreover the increase of elongation to failure, both at room and high temperature, was a further benefit of Mo addition and was a consequence of the absence of brittle  $\beta$ -Al<sub>5</sub>FeSi, which often acts as a crack nucleation site.

Air cooled samples exhibited lower values of YS and UTS at room temperature compared to the quenched ones, but reached similar performances after high temperature exposure.

These data supported the hypothesis of employing the alloy for high temperature application only after solution treatment, followed by air cooling, in order to avoid critical aspects linked to quench (see chapter 3.7.1).

### **3.9 Fractography**

Representative SEM micrographs of tensile fracture surfaces of samples with and without Mo, tested at room and 250°C, are reported in figs. 3.31 and 3.32, which highlight that fracture surfaces may be described by the same fracture mechanisms, involving cracking of eutectic Si and intermetallic particles, microcracks forming by joining adjacent cracked particles, subsequent linkage of cracks, leading to propagation and final fracture.

Fracture surfaces of samples tested at 250°C, however, showed higher ductility with dimples and tear ridges fig. 3.32.

Some shrinkage porosities were also observed (fig. 3.31d) and those could justify the lower UTS value of MoT samples, compared to A-T6 ones. In fact, while YS is slightly affected by casting defects, UTS is strongly influenced by microstructural defects, such as pores [3, 5].

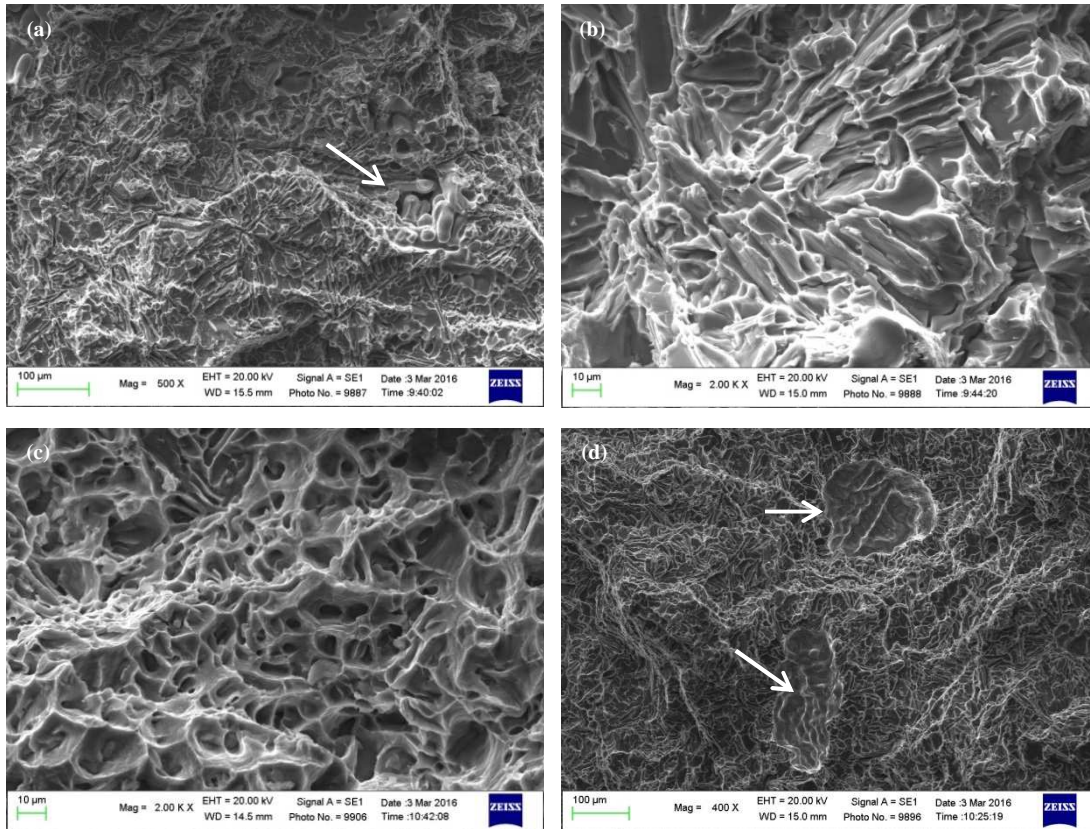


Figure 3.31 – SEM micrographs of fracture surface of (a,b) A354 and (c,d) A354+0.3%Mo alloys tested at room temperature. A large defect in (a) and macroporosity in (b) are highlighted by arrows

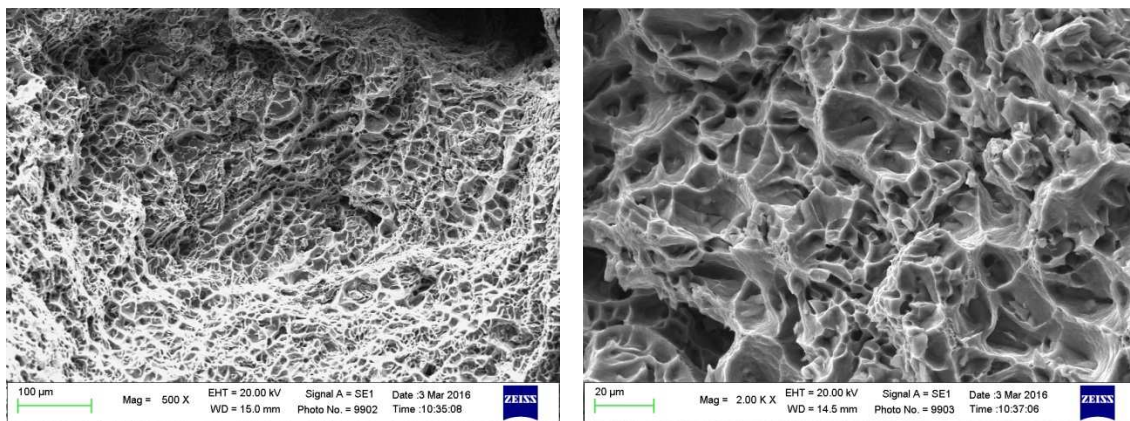


Figure 3.32 - SEM micrograph of fracture surface of A354+0.3%Mo alloy tested at high temperature (MoA sample)

## Chapter 4 - Conclusions

The results of this study highlight that the addition of Mo to Al-Si-Cu-Mg casting alloys could be effective in improving high temperature behaviour. In particular it was possible to define:

- Casting parameters able to guarantee an homogeneous distribution of Mo in casts
- Minimum Mo content  
Optimal Mo percentage alloy was identified as 0.3% wt. Higher quantities don't induce further properties enhancement and lead to cluster formation of Mo intermetallics
- Aging curves and heat treatment parameters for the modified alloys, in order to obtain an increase of mechanical properties after high temperature exposition.  
Solution treatment at 540°C had positive effects on following ageing stage and on mechanical properties of solubilised alloys, probably as a consequence of molybdenum dispersoids formation.  
Modified alloy heat treated according to new parameters highlighted an increase of strength both at room and 250°C of about 10% respect to traditional A354
- The effects of Mo addition on microstructure in particular on: eutectic silicon morphology and iron based intermetallics amount.  
In Mo-containing alloy the eutectic silicon was not completely modified, but no  $\beta$ -Al<sub>5</sub>FeSi particles were observed. These compounds reduce material performances due to their needle-like morphology, and their absence could explain the higher elongation to failure of the modified alloy respect to the traditional one

The research activity will be focused on the study of Mo based dispersoids precipitation sequence, by means of transmission electron microscopy (TEM), in order to further optimize the heat treatment parameters.

# Appendix

## Chapter 2 – Material and methods

### 2.5 Heat treatment

Acronym	Alloy	Heat treatment
A515T	A354	Solution treatment (495°C for 6h + 515°C for 2h) + quench (water at 60°C)
A515I	A354	Solution treatment (495°C for 6h + 515°C for 2h) + quench (water at 60°C) + ageing (180°C for 4h)
A540A	A354	Solution treatment (495°C for 6h + 540°C for 1h) + air cooling
A540T	A354	Solution treatment (495°C for 6h + 540°C for 1h) + quench (water at 60°C)
A540I	A354	Solution treatment (495°C for 6h + 540°C for 1h) + quench (water at 60°C) + ageing (180°C for 4h)
A540-10A	A354	Solution treatment (495°C for 6h + 540°C for 10h) + air cooling
A540-10T	A354	Solution treatment (495°C for 6h + 540°C for 10h) + quench (water at 60°C)
A540-10I	A354	Solution treatment (495°C for 6h + 540°C for 10h) + quench (water at 60°C) + ageing (180°C for 4h)
A01-515T	A354 + 0.1%Mo	Solution treatment (495°C for 6h + 515°C for 2h) + quench (water at 60°C)
A01-515I	A354 + 0.1%Mo	Solution treatment (495°C for 6h + 515°C for 2h) + quench (water at 60°C) + ageing (180°C for 4h)
A01-540A	A354 + 0.1%Mo	Solution treatment (495°C for 6h + 540°C for 1h) + air cooling

<b>A01-540T</b>	A354 + 0.1%Mo	Solution treatment (495°C for 6h + 540°C for 1h) + quench (water at 60°C)
<b>A01-540I</b>	A354 + 0.1%Mo	Solution treatment (495°C for 6h + 540°C for 1h) + quench (water at 60°C) + ageing (180°C for 4h)
<b>A01-540-10A</b>	A354 + 0.1%Mo	Solution treatment (495°C for 6h + 540°C for 10h) + air cooling
<b>A01-540-10T</b>	A354 + 0.1%Mo	Solution treatment (495°C for 6h + 540°C for 10h) + quench (water at 60°C)
<b>A01-540-10I</b>	A354 + 0.1%Mo	Solution treatment (495°C for 6h + 540°C for 10h) + quench (water at 60°C) + ageing (180°C for 4h)
<b>A03-515T</b>	A354 + 0.3%Mo	Solution treatment (495°C for 6h + 515°C for 2h) + quench (water at 60°C)
<b>A03-515I</b>	A354 + 0.3%Mo	Solution treatment (495°C for 6h + 515°C for 2h) + quench (water at 60°C) + ageing (180°C for 4h)
<b>A03-540A</b>	A354 + 0.3%Mo	Solution treatment (495°C for 6h + 540°C for 1h) + air cooling
<b>A03-540T</b>	A354 + 0.3%Mo	Solution treatment (495°C for 6h + 540°C for 1h) + quench (water at 60°C)
<b>A03-540I</b>	A354 + 0.3%Mo	Solution treatment (495°C for 6h + 540°C for 1h) + quench (water at 60°C) + ageing (180°C for 4h)
<b>A03-540-10A</b>	A354 + 0.3%Mo	Solution treatment (495°C for 6h + 540°C for 10h) + air cooling
<b>A03-540-10T</b>	A354 + 0.3%Mo	Solution treatment (495°C for 6h + 540°C for 10h) + quench (water at 60°C)
<b>A03-540-10I</b>	A354 + 0.3%Mo	Solution treatment (495°C for 6h + 540°C for 10h) + quench (water at 60°C) + ageing (180°C for 4h)
<b>A05-515T</b>	A354 + 0.5%Mo	Solution treatment (495°C for 6h + 515°C for 2h) + quench (water at 60°C)

<b>A05-515I</b>	A354 + 0.5%Mo	Solution treatment (495°C for 6h + 515°C for 2h) + quench (water at 60°C) + ageing (180°C for 4h)
<b>A05-540A</b>	A354 + 0.5%Mo	Solution treatment (495°C for 6h + 540°C for 1h) + air cooling
<b>A05-540T</b>	A354 + 0.5%Mo	Solution treatment (495°C for 6h + 540°C for 1h) + quench (water at 60°C)
<b>A05-540I</b>	A354 + 0.5%Mo	Solution treatment (495°C for 6h + 540°C for 1h) + quench (water at 60°C) + ageing (180°C for 4h)
<b>A05-540-10A</b>	A354 + 0.5%Mo	Solution treatment (495°C for 6h + 540°C for 10h) + air cooling
<b>A05-540-10T</b>	A354 + 0.5%Mo	Solution treatment (495°C for 6h + 540°C for 10h) + quench (water at 60°C)
<b>A05-540-10I</b>	A354 + 0.5%Mo	Solution treatment (495°C for 6h + 540°C for 10h) + quench (water at 60°C) + ageing (180°C for 4h)
<b>A08-515T</b>	A354 + 0.8%Mo	Solution treatment (495°C for 6h + 515°C for 2h) + quench (water at 60°C)
<b>A08-515I</b>	A354 + 0.8%Mo	Solution treatment (495°C for 6h + 515°C for 2h) + quench (water at 60°C) + ageing (180°C for 4h)
<b>A08-540A</b>	A354 + 0.8%Mo	Solution treatment (495°C for 6h + 540°C for 1h) + air cooling
<b>A08-540T</b>	A354 + 0.8%Mo	Solution treatment (495°C for 6h + 540°C for 1h) + quench (water at 60°C)
<b>A08-540I</b>	A354 + 0.8%Mo	Solution treatment (495°C for 6h + 540°C for 1h) + quench (water at 60°C) + ageing (180°C for 4h)
<b>A08-540-10A</b>	A354 + 0.8%Mo	Solution treatment (495°C for 6h + 540°C for 10h) + air cooling
<b>A08-540-10T</b>	A354 + 0.8%Mo	Solution treatment (495°C for 6h + 540°C for 10h) + quench (water at 60°C)

<b>A08-540-10I</b>	A354 + 0.8%Mo	Solution treatment (495°C for 6h + 540°C for 10h) + quench (water at 60°C) + ageing (180°C for 4h)
--------------------	---------------	--

Table A.1 – Schematization of heat treatment to which A354 alloy with different percentages of molybdenum were subjected and correspondent recognition acronym

## Chapter 3 - Results

### 3.2 Heat treatment

- A354+0.3%Mo air cooled:

Heat treatment	Time (h)	Hardness (HB10)
A354+0.3%Mo AC	0	78 ± 3
A354+0.3%Mo solub.495°C 6h + air cooling	6	74 ± 1
A354+0.3%Mo solub.495°C 6h+540°C 0.5h + air cooling	6,5	75 ± 4
A354+0.3%Mo solub.495°C 6h+540°C 1h + air cooling	7	75 ± 4
A354+0.3%Mo solub.495°C 6h+540°C 3h + air cooling	9	75 ± 4
A354+0.3%Mo solub.495°C 6h+540°C 5h + air cooling	11	74 ± 3
A354+0.3%Mo solub.495°C 6h+540°C 7h + air cooling	13	73 ± 1
A354+0.3%Mo solub.495°C 6h+540°C 15h + air cooling	23	72 ± 1
A354+0.3%Mo solub.495°C 6h+540°C 24h + air cooling	30	71 ± 1

Table A.2 - Hardness trend over solution treatment time of air cooled A354+0.3%Mo

- A354+0.3%Mo quenched:

Heat treatment	Time (h)	Hardness (HB10)
A354+0.3%Mo AC	0	78 ± 3
A354+0.3%Mo solub.495°C 6h + quench	6	76 ± 2
A354+0.3%Mo solub.495°C 6h+540°C 0.5h + quench	6,5	81 ± 2
A354+0.3%Mo solub.495°C 6h+540°C 1h + quench	7	84 ± 3
A354+0.3%Mo solub.495°C 6h+540°C 3h + quench	9	83 ± 3
A354+0.3%Mo solub.495°C 6h+540°C 5h + quench	11	82 ± 1
A354+0.3%Mo solub.495°C 6h+540°C 7h + quench	13	80 ± 3
A354+0.3%Mo solub.495°C 6h+540°C 15h + quench	23	78 ± 2
A354+0.3%Mo solub.495°C 6h+540°C 24h + quench	30	81 ± 1

Table A.3 - Hardness trend over solution treatment time of quenched A354+0.3%Mo

### 3.5 Hardness measurement

#### 3.5.1 Macrohardness measurements

- A354:

Tipo di lega	Durezza (HB10)
A354 Sr AC	86 ± 3
A354 sol.495°C 6h + air cooling	64 ± 1
A354 sol.495°C 6h + quench	64.3 ± 0.5

A354 solub. 495°C 6h + 540°C 1h + air cooling	82 ± 4
A354 solub. 495°C 6h + 540°C 1h + quench (water at 60°C)	83 ± 1

Table A.4 – Macrohardness values of A354 after every stage of heat treatment

- A354 + 0.1%Mo:

Tipo di lega	Durezza (HB10)
A354 Sr AC	79.0 ± 0.5
A354 + 0.1% Mo AC	79 ± 2
A354 + 0.1% Mo solub.495°C 6h+ quench (water at 60°C)	64 ± 2
A354 + 0.1% Mo solub.495°C 6h + 515°C 2h + quench (water at 60°C)	69 ± 2
A354 + 0.1% Mo solub.495°C 6h + 540°C 1h + quench (water at 60°C)	78 ± 1

Table A.5 – Macrohardness values of A354+0.1%Mo after every stage of heat treatment

- A354 + 0.3%Mo:

Tipo di lega	Durezza (HB10)
A354 Sr AC	79.0 ± 0.5
A354 + 0.3% Mo AC	85 ± 3
A354 + 0.3% Mo solub.495°C 6h+ quench (water at 60°C)	69.7 ± 0.4
A354 + 0.3% Mo solub.495°C 6h + 515°C 2h + quench (water at 60°C)	73 ± 1

A354 + 0.3% Mo solub.495°C 6h+540°C 1h + quench (water at 60°C)	99 ± 2
--	--------

Table A.6 – Macrohardness values of A354+0.3%Mo after every stage of heat treatment

- A354 + 0.5%Mo:

Tipo di lega	Durezza (HB10)
A354 Sr AC	79.0 ± 0.5
A354 + 0.5% Mo AC	90 ± 4
A354 + 0.5% Mo solub.495°C 6h+ quench (water at 60°C)	71 ± 1
A354 + 0.5% Mo solub.495°C 6h+515°C 2h + quench (water at 60°C)	77 ± 1
A354 + 0.5% Mo solub.495°C 6h+540°C 1h + quench (water at 60°C)	86 ± 1

Table A.7 – Macrohardness values of A354+0.5%Mo after every stage of heat treatment

- A354 + 0.8%Mo:

Tipo di lega	Durezza (HB10)
A354 Sr AC	79.0 ± 0.5
A354 + 0.8% Mo AC	82 ± 2
A354 + 0.8% Mo solub.495°C 6h+ quench (water at 60°C)	76 ± 1
A354 + 0.8% Mo solub.495°C 6h+515°C 2h + quench (water at 60°C)	73 ± 1
A354 + 0.8% Mo solub.495°C 6h+540°C 1h	79 ± 1

+ air cooling	
A354 + 0.8% Mo solub.495°C 6h+ 540°C 1h + quench (water at 60°C)	93 ± 1

Table A.8 – Macrohardness values of A354+0.1%Mo after every stage of heat treatment

### 3.5.2 Microhardness measurements

- A354 + 0.1%Mo:

Tipo di lega	Durezza (HB10)
A354 + 0.1% Mo AC	83 ± 11
A354 + 0.1% Mo solub.495°C 6h+ quench (water at 60°C)	68 ± 8
A354 + 0.1% Mo solub.495°C 6h+ 515°C 2h + quench (water at 60°C)	75 ± 6
A354 + 0.1% Mo solub.495°C 6h+ 540°C 1h + quench (water at 60°C)	86 ± 5

Table A.9 – Microhardness values of A354+0.1%Mo after every stage of heat treatment

- A354 + 0.3%Mo:

Tipo di lega	Durezza (HB10)
A354 + 0.3% Mo AC	78 ± 10
A354 + 0.3% Mo solub.495°C 6h+ quench (water at 60°C)	80 ± 7
A354 + 0.3% Mo solub.495°C 6h+ 515°C 2h + quench (water at 60°C)	80 ± 6
A354 + 0.3% Mo solub.495°C 6h+ 540°C 1h	81 ± 9

+ quench (water at 60°C)

**Table A.10 – Microhardness values of A354+0.3%Mo after every stage of heat treatment**

- A354 + 0.5%Mo:

<b>Tipo di lega</b>	<b>Durezza (HB10)</b>
A354 + 0.5% Mo AC	70 ± 10
A354 + 0.5% Mo solub.495°C 6h+ quench (water at 60°C)	74 ± 4
A354 + 0.5% Mo solub.495°C 6h + 515°C 2h + quench (water at 60°C)	71 ± 8
A354 + 0.5% Mo solub.495°C 6h + 540°C 1h + quench (water at 60°C)	79 ± 6

**Table A.11 – Microhardness values of A354+0.5%Mo after every stage of heat treatment**

- A354 + 0.8%Mo:

<b>Tipo di lega</b>	<b>Durezza (HB10)</b>
A354 + 0.8% Mo AC	59 ± 11
A354 + 0.8% Mo solub.495°C 6h+ quench (water at 60°C)	68 ± 6
A354 + 0.8% Mo solub.495°C 6h + 515°C 2h + quench (water at 60°C)	57 ± 1
A354 + 0.8% Mo solub.495°C 6h + 540°C 1h + air cooling	71 ± 4
A354 + 0.8% Mo solub.495°C 6h + 540°C 1h + quench (water at 60°C)	77 ± 7

**Table A.12 – Microhardness values of A354+0.8%Mo after every stage of heat treatment**

## References

- [1] I. J. Polmear, *Light alloys – From traditional alloys to nanocrystals* (fourth edition), Butterworth-Heinemann, 2006
- [2] M. Fabris, “Analisi difettologica e metallurgica nella produzione di ruote in lega leggera”, Tesi di laurea in Ingegneria Meccanica – Innovazione del Prodotto, Università degli studi di Padova, A.A. 2012-2013
- [3] A. J. Plotkowski, “Refinement of the Cast Microstructure of Hypereutectic Aluminum-Silicon Alloys with an Applied Electric Potential”, Master of Science in Engineering, Grand Valley State University, 2012
- [4] Keith E. Knipling, David C. Dunand, and David N. Seidman (2006). Criteria for developing castable, creep-resistant aluminum-based alloys – A review. *Zeitschrift für Metallkunde*: Vol. 97, No. 3, pp. 246-265
- [5] R. S. Rana, Rajesh Purohit, and S Das, “Reviews on the Influences of alloying elements on the microstructure and mechanical properties of aluminum alloys and aluminum composites”, *International Journal of Scientific and Research Publications*, Volume 2, Issue 6, June 2012 ISSN 2250-3153
- [6] Meng Sha, Shusen Wu, Xingtao Wang, Li Wan, Ping An, “Effects of cobalt content on microstructure and mechanical properties of hypereutectic Al–Si alloys”, *Materials Science and Engineering A* 535 (2012) 258–263
- [7] Erik Oberg, Franklin Jones, Holbrook Horton, Henry Ryffel and Christopher McCauley, “*Machinery's Handbook 29th Edition*”, Industrial Press (2012)
- [8] J. Gilbert Kaufman, Elwin L. Rooy, “*Aluminum Alloy Castings Properties, Processes, and Applications*”, ASM International (2004)
- [9] E. Sjölander, “Heat treatment of Al-Si-Cu-Mg casting alloys”, Master of Science in Mechanical Engineering, School of Engineering, Jönköping University, 2011
- [10] A.M.A. Mohamed and F.H. Samuel, “A Review on the Heat Treatment of Al-Si-Cu/Mg Casting Alloys”, *Intech open science| open minds*, 2012
- [11] Aniruddha Biswas, Donald J. Siegel, David N. Seidman, “Compositional evolution of Q-phase precipitates in an aluminum alloy”, *Acta Materialia* 75 (2014) 322–336
- [12] J. Hernandez-Sandoval, G.H. Garza-Elizondo, A.M. Samuel, S. Valtierra, F.H. Samuel, “The ambient and high temperature deformation behavior of Al–Si–Cu–Mg alloy with minor Ti, Zr, Ni additions”, *Materials and Design* 58 (2014) 89–101
- [13] A.R. Farkoosh, M. Javidani, M. Hoseini, D. Larouche M. Pekguleryuz, “Phase formation in as-solidified and heat-treated Al–Si–Cu–Mg–Ni alloys: Thermodynamic assessment and experimental investigation for alloy design”, *Journal of Alloys and Compounds* 551 (2013) 596–606
- [14] H. Okamoto, “Al-Ni (Aluminum-Nickel)”, *Journal of phase equilibria* Vol. 14 No.2 (1993)
- [15] A.M.A.Mohamed, F.H.Samuel Saleh Al kahtani, “Microstructure, tensile properties and fracture behavior of high temperature Al–Si–Mg–Cu cast alloys”, *Materials Science & Engineering A* 577 (2013) 64–72
- [16] Daniele Casari, Thomas H.Ludwig, Mattia Merlin, Lars Arnberg, Gian Luca Garagnani, “The effect of Ni and V trace elements on the mechanical properties of A356 aluminium foundry alloy in as-cast and T6 heat treated conditions”, *Materials Science & Engineering A* 610 (2014) 414–426
- [17] J. Murray, A. Peruzzi, J.P. Abriata, “The Al-Zr (aluminum-zirconium) system”, *Journal of phase equilibria* Vol. 13 No.3 (1992)

- [18] Keith E. Knippling, David N. Seidman, David C. Dunand, "Ambient- and high-temperature mechanical properties of isochronally aged Al-0.06Sc, Al-0.06Zr and Al-0.06Sc-0.06Zr (at.%) alloys", *Acta Materialia* 59 (2011) 943–954
- [19] Wojciech Kasprzak, Babak Shalchi Amirkhiz, Marek Niewczas, "Structure and properties of cast Al-Si based alloy with Zr-V-Ti additions and its evaluation of high temperature performance", *Journal of Alloys and Compounds* 595 (2014) 67–79
- [20] R. Mahmudi, P. Sepehrband, H.M. Ghasemi, "Improved properties of A319 aluminum casting alloy modified with Zr", *Materials Letters* 60 (2006) 2606–2610
- [21] S.K. Shaha, F. Czerwinski, W. Kasprzak, J. Friedman, D.L. Chen, "Thermal stability of (AlSi)<sub>x</sub>(ZrVTi) intermetallic phases in the Al-Si-Cu-Mg cast alloy with additions of Ti, V, and Zr", *Thermochimica Acta* 595 (2014) 11–16
- [22] A.R.Farkoosh, X.Grant Chen, M.Pekguleryuz, "Dispersoid strengthening of a high temperature Al-Si-Cu-Mg alloy via Mo addition", *Materials Science & Engineering A620* (2015) 181–189
- [23] A.R.Farkoosh, X.Grant Chen, M.Pekguleryuz, "Interaction between molybdenum and manganese to form effective dispersoids in an Al-Si-Cu-Mg alloy and their influence on creep resistance", *Materials Science & Engineering A627* (2015) 127–138
- [24] H. R. Ammar, A. M. Samuel, F. H. Samuel, E. Simielli, G. K. Sigworth, J. C. Lin., "Influence of aging parameters on the tensile properties and Quality Index of Al-9Si-1.8Cu-0.5Mg 354 type casting alloys", *Metallurgical and Materials Transactions A*, January 2012, Volume 43, Issue 1, pp 61-73
- [25] Sjölander et al., "Optimization of Solution Treatment of Cast Al-7Si-0.3Mg and Al-8Si-3Cu-0.5Mg alloys", *Metallurgical and Materials Transactions. A*, ISSN 1073-5623, E-ISSN 1543-1940, Vol. 45, no 4, 1916-1927 p. (2013)

## Acknowledgments

Sì, lo so. Dopo una tesi interamente in inglese vi sareste aspettati anche i ringraziamenti in lingua e invece, un po' per la fretta, un po' per piacere mio, almeno questa parte sarà in italiano.

Prima di tutto vorrei ringraziare il Dipartimento di metallurgia della facoltà di Ingegneria industriale, per avermi dato l'opportunità di vivere questo tipo di esperienza all'interno della propria struttura.

Ringrazio di cuore il prof. Morri per avermi reso partecipe delle attività di ricerca, coinvolgendomi attivamente nel lavoro e dimostrandomi attenzione nonostante i numerosi impegni.

Un grazie particolare va a Stefania, che mi ha dovuto sopportare più di tutti gli altri, mi ha seguito passo passo nello svolgimento del lavoro e mi ha permesso di migliorare il mio metodo.

Un ringraziamento speciale va inoltre al prof. Caretti, il quale è riuscito a districare una situazione complicata creatasi a monte, che non dovrebbe mai capitare ad uno studente.

Vorrei ringraziare i miei genitori che mi hanno permesso di studiare e che mi hanno sempre sostenuto in tutto ciò che faccio.

Un grazie è d'obbligo anche per i miei amici, che hanno alleggerito il peso degli anni a Bologna e soprattutto per Atena, che più degli altri ho stressato negli ultimi mesi.

Vorrei ringraziare inoltre il Trio Medusa, senza i quali i viaggi in treno la mattina sarebbero stati interminabili e tristi.

Un grazie meno serio va inoltre al durometro ed alle lappatrici, compagni fedeli di tante disavventure, che mi hanno tenuto compagnia per intere giornate senza mai abbandonarmi.

Infine, apparirà strano, ma vorrei ringraziare il corso di “Chimica e tecnologie per l'ambiente e i materiali – Curriculum materiali tradizionali e innovativi” di Faenza, perché in fondo quello che so fare e che in parte sono, lo devo anche ad esso.

A tutti voi va comunque il mio più sentito ringraziamento, perché in un modo o nell'altro mi avete permesso di svolgere e portare a termine questo lavoro.